

A Virtual Finite Element Method for Two Dimensional Maxwell Interface Problems with a Background Unfitted Mesh

Shuhao Cao

*Department of Mathematics and Statistics, Washington University in St. Louis
St. Louis, MO 63130
s.cao@wustl.edu*

Long Chen

*Department of Mathematics, University of California Irvine
Irvine, CA 92697
chenlong@math.uci.edu*

Ruchi Guo

*Department of Mathematics, University of California Irvine
Irvine, CA 92697
ruchig@uci.edu*

A virtual element method (VEM) with the first order optimal convergence order is developed for solving two dimensional Maxwell interface problems on a special class of polygonal meshes that are cut by the interface from a background unfitted mesh. A novel virtual space is introduced on a virtual triangulation of the polygonal mesh satisfying a maximum angle condition, which shares exactly the same degrees of freedom as the usual $\mathbf{H}(\text{curl})$ -conforming virtual space. This new virtual space serves as the key to prove that the optimal error bounds of the VEM are independent of high aspect ratio of the possible anisotropic polygonal mesh near the interface.

Keywords: Virtual elements; Maxwell interface problems; $\mathbf{H}(\text{curl})$ -elliptic equations; anisotropic error analysis

AMS Subject Classification: 65N12, 65N15, 65N30, 46E35

1. Introduction

Maxwell interface problems widely appear in a large variety of science and engineering applications. In this article, we propose a virtual element method (VEM) to solve a two-dimensional (2D) $\mathbf{H}(\text{curl}; \Omega)$ -elliptic interface problem that is originated from Maxwell equations. One distinct advantage of the proposed method is its flexibility on the mesh generation to cater the interface. The mesh for computation is obtained from a background unfitted mesh by cutting interface elements into triangles and quadrilaterals, and the optimal convergence order is guaranteed independent of the mesh anisotropy.

To describe the idea, we let $\Omega \subseteq \mathbb{R}^2$ be a bounded domain and let $\Gamma \subseteq \Omega$ be a smooth interface curve, as illustrated by the left plot in Figure 2.1. The interface

2 Authors' Names

Γ cuts Ω into two subdomains Ω^\pm occupied by media with different magnetic and electric properties. We consider the following $\mathbf{H}(\text{curl}; \Omega)$ -elliptic interface problem for the electric field $\mathbf{u} : \Omega \rightarrow \mathbb{R}^2$:

$$\underline{\text{curl}} \alpha \text{curl} \mathbf{u} + \beta \mathbf{u} = \mathbf{f} \quad \text{in } \Omega = \Omega^- \cup \Omega^+, \quad (1.1a)$$

with $\mathbf{f} \in \mathbf{L}^2(\Omega)$, subject to the Dirichlet boundary condition:

$$\mathbf{u} \cdot \mathbf{t} = 0 \quad \text{on } \partial\Omega, \quad (1.1b)$$

where the operator curl is for vector functions $\mathbf{v} = (v_1, v_2)^\top$ such that $\text{curl} \mathbf{u} = \partial_{x_1} v_2 - \partial_{x_2} v_1$ while $\underline{\text{curl}}$ is for scalar functions v such that $\underline{\text{curl}} v = (\partial_{x_2} v, -\partial_{x_1} v)^\top$ with “ \top ” denoting the transpose herein. The coefficients $\alpha = \alpha^\pm$ and $\beta = \beta^\pm$ in Ω^\pm are assumed to be positive piecewise constant functions of which the locations of the discontinuity align with one another. Moreover, we consider the following jump conditions at the interface Γ :

$$[\mathbf{u} \cdot \mathbf{t}]_\Gamma := \mathbf{u}^+ \cdot \mathbf{t} - \mathbf{u}^- \cdot \mathbf{t} = 0, \quad (1.1c)$$

$$[\alpha \underline{\text{curl}} \mathbf{u}]_\Gamma := \alpha^- \underline{\text{curl}} \mathbf{u}^+ - \alpha^+ \underline{\text{curl}} \mathbf{u}^- = 0, \quad (1.1d)$$

where \mathbf{t} denotes a tangential vector to Γ . The condition (1.1c) is due to the tangential continuity of $\mathbf{H}(\text{curl})$ functions and (1.1d) is from the fact that $H(\underline{\text{curl}})$ is isomorphic to H^1 in 2D. The interface model (1.1) arises from each time step in a stable time-marching scheme for the eddy current computation of Maxwell equations [2, 4]. In this model, α denotes the magnetic permeability and $\beta \sim \sigma/\Delta t$ is the scaling of the conductivity σ by the time-marching step size Δt .

For Maxwell equations, $H(\text{curl})$ -conforming Nédélec finite element spaces are widely used [17, 25, 37]. As for interface problems, the authors in [26] analyze the standard finite element methods (FEMs) for $\mathbf{H}(\text{curl})$ -elliptic equations. The semi-discrete analysis for Maxwell interface problems with low regularity is provided in [43]. In addition, due to the potentially low regularity, there are many works focusing on developing a posteriori error estimators and adaptive FEM [8, 16, 22].

Numerical methods for solving interface problems based on unfitted meshes are attractive since they circumvent the burden of generating high-quality interface-fitted meshes which may be time-consuming for three dimensions (3D) or for moving interface problems. There have been a lot of works in this field on solving H^1 -elliptic interface problems, see [7, 23, 33] and the reference therein. However, there are much fewer works on solving Maxwell interface problems. Typical examples include matched interface and boundary (MIB) formulation [44], adaptive FEMs [15], and non-matching mesh methods [10, 11, 14]. Recently, a penalty method is developed in [35] requiring higher regularity.

A main difficulty for solving $\mathbf{H}(\text{curl})$ problems comes from low regularity of the exact solution, even for our assumption $\mathbf{u} \in \mathbf{H}^1(\text{curl}; \Omega) := \{\mathbf{u} \in \mathbf{H}^1(\Omega), \text{curl} \mathbf{u} \in H^1(\Omega)\}$. The expected optimal convergence rate highly relies on the conformity of approximation spaces due to the $\mathcal{O}(h^{1/2})$ approximation order on boundary of

elements for functions in $\mathbf{H}^1(\text{curl}; \Omega)$, see specifically [38, Lemma 5.52]. For example, when solving Maxwell equations by discontinuous Galerkin (DG) methods [27, 28, 29], penalties are in general needed on boundary of elements due to the non-conformity of DG spaces, and the standard argument directly applying the trace inequalities may only yield suboptimal convergence rates. Instead, the analysis approaches in [27, 28, 29] employ a $\mathbf{H}(\text{curl})$ -conforming subspace of the broken DG space to overcome this issue.

This essential difficulty will make the development of optimal convergent unfitted mesh methods for Maxwell interface problems especially challenging since almost all the unfitted mesh methods aforementioned use non-conforming spaces for approximation, and it is unclear whether conforming subspaces with sufficient approximation capabilities exist such that the approaches in [27, 28, 29] can be applied. Indeed, Hiptmair et al. in [10, 11] show that using Nitsche's penalties on interface edges can only yield suboptimal convergence rates in both computation and analysis. Recently, this issue was further explored numerically in [41]. An alternative approach is to use immersed finite element methods in a Petrov-Galerkin formulation [24], where the standard conforming Nédélec space is used as the test function space to remove the non-conformity errors. However, the resulted matrix may not be symmetric anymore, which could cause troubles for fast solvers especially for 3D Maxwell equations.

Motivated by the works [9, 13], we believe that the virtual element method (VEM) provides a new direction to solve Maxwell interface problems that can achieve optimal convergence on (background) unfitted meshes. The VEM was first introduced in [5] to solve H^1 -elliptic equations where the H^1 -virtual space consists of shape functions constructed by solving local problems on elements with general polygonal shapes. The $\mathbf{H}(\text{curl})$ -conforming virtual space was then introduced in [19, 20] to solve magnetostatic problems. As one attractive feature, the underling virtual space for approximation is always conforming on an almost arbitrary polygonal mesh of the computation domain. It is our key motivation to use it for solving Maxwell interface problems on meshes that are generated from a background unfitted mesh. However, different from [19, 20] that use a special mixed formulation [31], in this work we shall employ the standard $\mathbf{H}(\text{curl})$ -elliptic equation (1.1a) as the model problem. Very recently, a similar VEM for Maxwell equations with the lowest order and shape-regular meshes is analyzed in [21]. Compared with [21], our results focus more on the discretization's robustness to the shape of elements, while the analysis only relies on mature simplicial finite element tools.

In our analysis, the key to achieve the optimal error bound regardless of element shapes is a novel virtual element space that shares exactly the same degrees of freedom of the one invented in [19, 20], and thus preserves all its information including the same projection and curl values for computation. This space is constructed as a subspace of the standard Nédélec space on a further (virtual) triangulation of the polygonal mesh that satisfies a maximum angle condition [1]. Locally on each

4 Authors' Names

polygonal element, the new virtual functions can be also considered as discrete harmonic extensions according to the boundary conditions (degrees of freedom), while the usual virtual functions in [19, 20] may be considered as continuous extensions. As the key advantage of using this new space, we are able to establish local Poincaré-type inequalities and optimal approximation capabilities for a large class of polygonal-shape elements all independent of element anisotropy which are the crucial intermediate results toward the final optimal error bound. A related work is [16] that constructs sub-meshes on interface elements of a background unfitted mesh for computation. One essential difference between the proposed method and [16] is that the virtual mesh and space are only used for analysis in our work, while the computation procedure is the same as the usual VEM with the lowest order. The convergence is guaranteed independent of the element shape provided that the background mesh is shape-regular.

This article consists of 5 additional sections. In the next section, we introduce the background unfitted mesh and the fitted mesh according to interface geometry. In Section 3, we describe virtual spaces and projection operators. In Section 4, we present the numerical scheme and derive the error equation. In Section 5, we estimate the interpolation errors. In Section 6, we show that the convergence is of optimal order. In the last section, some numerical examples are presented to verify the theoretical estimates.

2. Preliminaries

In this section, we first describe an unfitted background triangular mesh and then locally partition it into a fitted mesh used for computation. We then introduce Sobolev spaces for $H(\text{curl})$ -interface problems. Although the triangular and quadrilateral shape is the focus of this work, we highlight that most key results are actually established and presented for more general polygonal element shapes.

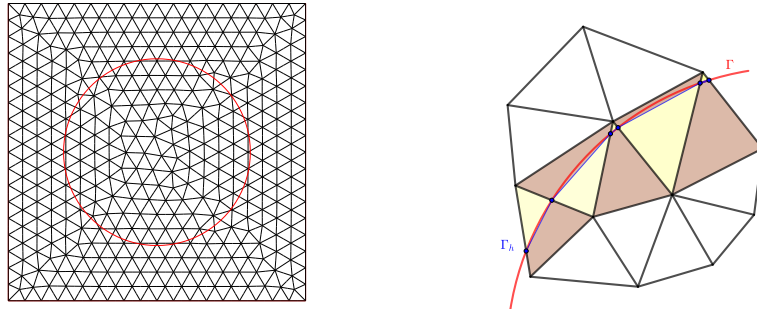


Fig. 2.1. Left: a background unfitted mesh. Right: interface elements in the unfitted mesh are further partitioned into quadrilateral and triangular elements, shaded by brown and yellow colors respectively.

Consider an interface-independent shape-regular triangular mesh of the domain Ω . Note that this mesh could be simply taken as a highly-structured mesh due to the interface independence. We shall call it a background mesh, and denoted it by \mathcal{T}_h^B . Another example of \mathcal{T}_h^B is a uniform Cartesian grid which is widely used for unfitted mesh methods. The proposed analysis approach can be easily adapt to this grid. If a triangular element in \mathcal{T}_h^B intersects the interface, then it is called an interface element. The collection of interface elements is denoted as \mathcal{T}_h^{Bi} . The remaining elements are called non-interface elements. For this background mesh, we further make the following assumptions:

- (A) Each interface element intersects with Γ at most two distinct points on two different edges.
- (B) Each interface element does not intersect with the boundary of Ω .

By this assumption (A), on an interface element $K \in \mathcal{T}_h^{Bi}$ we define Γ_h^K as the line connecting the two intersection points. Then all these connected small segments, defined as Γ_h , form a piecewise linear approximation of the true interface Γ . In addition, by the assumption (A), each triangular interface element K is cut by Γ_h^K into a triangular and a quadrilateral subelement from which an interface fitted mesh can be generated. We denote this fitted mesh by \mathcal{T}_h . The collections of quadrilateral and triangular elements in \mathcal{T}_h resulted by the interface-cutting are denoted by \mathcal{T}_h^q and \mathcal{T}_h^t , respectively. Those elements all have one edge aligning with the interface approximately, and thus are also called interface elements in \mathcal{T}_h . Clearly, there holds

$$\overline{\cup\{K \in \mathcal{T}_h^t \cup \mathcal{T}_h^q\}} = \overline{\cup\{K \in \mathcal{T}_h^{Bi}\}}.$$

Note that \mathcal{T}_h and \mathcal{T}_h^B are only different on the interface elements. Furthermore, an interface element K is assumed to be cut into K_h^- and K_h^+ by Γ_h^K , and the mismatch portion, with $K^\pm := K \cap \Omega^\pm$ cut from the original interface, is denoted by K_{int} , indicated by the shaded region in the left plot of Figure 2.2.

In addition, for each interface edge Γ_h^K , we assume there is a shape regular triangle $B_h^K \subseteq \Omega$ with the base Γ_h^K and a height $\mathcal{O}(h_K)$. Here B_h^K is not required to align with the elements in the mesh. Further assume all the B_h^K have finite overlapping. Note that for the considered background regular triangular mesh, for each interface element K , this B_h^K certainly exists and can be further shown to be contained in K .

Moreover we assume the interface is well-resolved by the mesh, and it can be quantitatively described in terms of the following lemma [23].

Lemma 2.1. *Suppose the mesh is sufficiently fine such that $h < h_0$ for some value h_0 , on each interface element $K \in \mathcal{T}_h^{Bi}$, there exist a constant C independent of the interface location inside K and h_K such that for every point $x \in \Gamma \cap K$ with its orthogonal projection x^\perp onto Γ_h^K ,*

$$\text{dist}(x, x^\perp) \leq Ch_K^2. \quad (2.1)$$

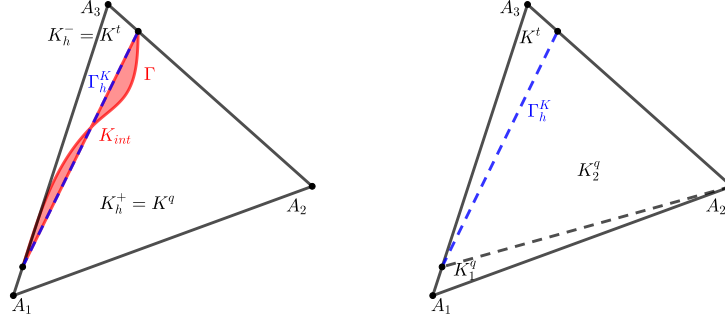


Fig. 2.2. Left: an interface element $K \in \mathcal{T}_h^B$ is cut to a triangular element K^t and a quadrilateral element K^q of which both are in \mathcal{T}_h . Right: the quadrilateral element is further cut into two triangular elements K_1^q and K_2^q .

The explicit dependence of h_0 on the curvature of the interface can be found in [23]. An adaptively-generated background mesh can be found in [42] capturing large curvature of interface curve. Now following [26, 34], we introduce the δ -strip:

$$S_\delta := \{x \in \Omega : \text{dist}(x, \Gamma) < \delta\}, \quad \text{and} \quad S_\delta^\pm := \{x \in \Omega^\pm : \text{dist}(x, \Gamma) < \delta\}. \quad (2.2)$$

By the estimate (2.1), we have

$$\cup \{K_{\text{int}} : K \in \mathcal{T}_h^{Bi}\} \subseteq S_\delta, \quad \delta \leq C_\Gamma h^2 \quad (2.3)$$

with the constant C_Γ only depending on the interface. Furthermore, from [26, 34] we can control the L^2 -norm in the δ -strip by the width of the strip and thus obtain first order convergence when $\delta = \mathcal{O}(h^2)$.

Lemma 2.2. *It holds for any $z \in H^1(\Omega^\pm)$ that*

$$\|z\|_{L^2(S_\delta^\pm)} \leq C\sqrt{\delta}\|z\|_{H^1(\Omega^\pm)}. \quad (2.4)$$

We next introduce some major Sobolev spaces used throughout this article. For each subdomain $\omega \subseteq \Omega$, we let $H^s(\omega)$ and $\mathbf{H}^s(\omega)$, $s \geq 0$, be the standard scalar and 2D vector Hilbert spaces on ω where specifically $H^0(\omega) = L^2(\omega)$ and $\mathbf{H}^0(\omega) = \mathbf{L}^2(\omega)$. In addition, for $s \geq 0$, we let

$$\mathbf{H}^s(\text{curl}; \omega) = \{\mathbf{v} \in \mathbf{H}^s(\omega) : \text{curl } \mathbf{v} \in H^s(\omega)\}. \quad (2.5)$$

Similarly, we introduce $\mathbf{H}^s(\text{div}; \omega)$ as the counterpart of $\mathbf{H}^s(\text{curl}; \omega)$ with the divergence operator. If $\omega \cap \Gamma \neq \emptyset$, then $\omega^\pm = \omega \cap \Omega^\pm$, and $\mathbf{H}^s(\text{curl}; \omega^- \cup \omega^+)$ denotes the space of functions piecewisely defined in $\mathbf{H}^s(\text{curl}; \omega^\pm)$. For these spaces, we can define their subspaces $H_0^s(\omega)$, $\mathbf{H}_0^s(\omega)$, and $\mathbf{H}_0^s(\text{curl}; \omega)$ with the zero trace on $\partial\omega$. Also let $(\cdot, \cdot)_\omega$ be the standard L^2 inner product on ω .

When the interface is smooth, the solution to the problem is expected to have an $\mathbf{H}^1(\text{curl}; \Omega^\pm)$ regularity ([18, 30]). The fundamental $\mathbf{H}^1(\text{curl}; \Omega)$ -extension operator

established by Hiptmair, Li and Zou in [26] (Theorem 3.4 and Corollary 3.5) will be used in analysis.

Theorem 2.1 (Theorem 3.4 and Corollary 3.5 in [26]). *There exist two bounded linear operators*

$$\mathbf{E}_{\text{curl}}^{\pm} : \mathbf{H}^1(\text{curl}; \Omega^{\pm}) \rightarrow \mathbf{H}^1(\text{curl}; \Omega) \quad (2.6)$$

such that for each $\mathbf{u} \in \mathbf{H}^1(\text{curl}; \Omega^{\pm})$:

1. $\mathbf{E}_{\text{curl}}^{\pm} \mathbf{u} = \mathbf{u}$ a.e. in Ω^{\pm} .
2. $\|\mathbf{E}_{\text{curl}}^{\pm} \mathbf{u}\|_{\mathbf{H}^1(\text{curl}; \Omega)} \leq C_E \|\mathbf{u}\|_{\mathbf{H}^1(\text{curl}; \Omega^{\pm})}$ with the constant C_E only depending on Ω and Γ .

Using these two special extension operators, we can define $\mathbf{u}_E^{\pm} = \mathbf{E}_{\text{curl}}^{\pm} \mathbf{u}^{\pm}$ which are the keys in the analysis later. Finally, throughout this article, for simplicity we shall use \lesssim to denote $\dots \leq C \dots$ with a generic constant independent of mesh size and interface location relative to the mesh.

3. Virtual Element Spaces

In this section, we shall introduce a virtual element space using the lowest order Nédélec element on a virtual triangulation which is obtained by refinement of the background mesh.

3.1. Virtual Edge Element Spaces

In the proposed method, triangular elements and quadrilateral elements in \mathcal{T}_h are treated differently. To avoid confusion, in this section we shall usually use K^t and K^q to denote triangular and quadrilateral elements in \mathcal{T}_h^t and \mathcal{T}_h^q , respectively, while K denotes an interface element in the background mesh \mathcal{T}_h^B or general elements in \mathcal{T}_h if there is no need to distinguish their shape. In addition, for simplicity's sake, we always use h_K as the diameter of elements K , K^q and K^t .

For any element or edge ω in \mathcal{T}_h , we let $\mathbb{P}_k(\omega)$ be the k -th degree polynomial space defined on ω . Given a triangle K , we shall consider the first family Nédélec element of the lowest degree [39] as the underling approximation space:

$$\mathcal{ND}_h(K) = \{\mathbf{a} + b(x_2, -x_1)^{\top} : \mathbf{a} \in \mathbb{R}^2, b \in \mathbb{R}\}. \quad (3.1)$$

Then (3.1) will be used on all the non-interface elements of \mathcal{T}_h^B (or \mathcal{T}_h) as well as the triangular interface elements K^t . But for K^q we need to employ a virtual element space. Let us first discuss the definition on a general polygon P :

$$\begin{aligned} \tilde{\mathcal{V}}_h(P) = \{ & \mathbf{v}_h \in \mathbf{H}(\text{curl}; P) \cap \mathbf{H}(\text{div}; P) : \mathbf{v}_h \cdot \mathbf{t}_e \in \mathbb{P}_0(e), \forall e \subset \partial P, \\ & \text{div}(\mathbf{v}_h) = 0, \text{curl}(\mathbf{v}_h) \in \mathbb{P}_0(P)\}. \end{aligned} \quad (3.2)$$

This is exactly the one introduced in [20, 19] with the lowest degree and $\mathcal{ND}_h(P) \subset \tilde{\mathcal{V}}_h(P)$. Similar to the ones for (3.1) defined on triangles, the local degrees of freedom

(d.o.f.) for (3.2) are

$$\mathbf{v}_h|_e \cdot \mathbf{t}_e, \quad e \subset \partial P. \quad (3.3)$$

It has been shown in [20, 19] that the functions in (3.2) can be uniquely determined by d.o.f. (3.3). For the present situation, $\tilde{V}_h(K^q)$ ($P = K^q$) is the space used for discretization on K^q .

As the shape of elements K^q could be very anisotropic, a robust norm equivalence and interpolation error estimate is hard to establish in $\tilde{V}_h(K^q)$. To address this issue, we shall introduce an auxiliary triangulation of Ω (a virtual mesh), and construct an auxiliary $\mathbf{H}(\text{curl})$ -conforming space associated with this mesh. Given an interface element $K \in \mathcal{T}_h^{Bi}$, with an quadrilateral subelement $K^q \in \mathcal{T}_h^q$, then the local auxiliary mesh is formed by a Delaunay triangulation of K^q : connecting the diagonal s.t. the sum of angles opposing to the diagonal is less than or equal to π ; see the right plot in Figure 2.2 for an illustration. Although it may contain anisotropic triangles, each triangle from this new partition satisfies the maximum angle condition (Lemma 3.1), which is key to robust interpolation error estimates (see Section 3.2). A similar result is proven in [13] for Cartesian grids.

Lemma 3.1. *Let K be a shape regular triangle, i.e., there exist $0 < \theta_{\min} \leq \theta_{\max} < \pi$ such that every angle θ in K satisfies $\theta_{\min} \leq \theta \leq \theta_{\max}$, then every triangle in the auxiliary Delaunay triangulation on K described above satisfies the maximum angle condition, i.e., every $\tilde{\theta}$ in the auxiliary triangulation is bounded above by $\tilde{\theta}_{\max} \leq \max\{\pi - \theta_{\min}, \theta_{\max}\}$.*

Proof. Without loss of generality, we consider the triangle in the right plot of Figure 2.2 for illustration where the left and right cutting points are D and E , respectively. We shall bound angles of three triangles: $K^t = \triangle DEA_3$, $K_1^q = \triangle A_1A_2D$, and $K_2^q = \triangle DA_2E$. If the angle is one of (or part of) the angles of $\triangle A_1A_2A_3$, then it is bounded by θ_{\max} . If the triangle contains one of the angles of $\triangle A_1A_2A_3$, as the sum of three angles is π , we conclude other angles are bounded by $\pi - \theta_{\min}$. So we only focus on angles of the triangle $\triangle DA_2E$.

Now use the Delaunay property, $\angle DEA_2 + \angle DA_1A_2 \leq \pi$, we get $\angle DEA_2 \leq \pi - \theta_{\min}$ and $\angle EDA_2 \leq \angle A_3DA_2 \leq \pi - \angle A_1A_3A_2 \leq \pi - \theta_{\min}$.

We thus have verified $\tilde{\theta}_{\max} \leq \max\{\pi - \theta_{\min}, \theta_{\max}\}$. \square

The discussion for the special case on a quadrilateral K^q is postponed to Section 5, and the results on a general polygon P are the focus in the rest of this section. To be able to establish a robust analysis of the approximation capabilities of $V_h(P)$ below and the stability of the discretization, P is assumed to admit a triangulation $\mathcal{T}_h(P)$ with no additional interior vertices added, i.e., the collection of edges $\mathcal{E}_h(P)$ in $\mathcal{T}_h(P)$ are solely formed by the vertices on ∂P , and this triangulation satisfies

- (P1) the maximum angle condition for each triangle in $\mathcal{T}_h(P)$;
- (P2) no-short-interior-edge condition: $h_P \lesssim |e|$ for every interior edge e ;

(P3) star-convexity: there exists $\mathbf{x} := (\bar{x}_1, \bar{x}_2) \in P$ such that $\overline{\mathbf{x}\mathbf{y}} \subseteq P$, $\forall \mathbf{y} \in \partial P$.

We then define an auxiliary VEM space

$$V_h(P) = \{\mathbf{v}_h \in \mathbf{H}(\text{curl}; P) : \mathbf{v}_h|_K \in \mathcal{ND}_h(K), \forall K \in \mathcal{T}_h(P), \\ \text{curl } \mathbf{v}_h \in \mathbb{P}_0(P)\}. \quad (3.4)$$

Indeed we can show the VEM space defined by (3.4) shares the same d.o.f. of (3.3).

Lemma 3.2. *Let P be a simple polygon, then the d.o.f. $\mathbf{v}_h \cdot \mathbf{t}_e$, $e \subseteq \partial P$ are unisolvent on the space $V_h(P)$.*

Proof. Let us consider the following well-posed problem: for any given boundary conditions $\mathbf{v}_h \cdot \mathbf{t}_e$, $e \in \partial P$, find $(\mathbf{v}_h, \lambda_h)$ satisfying

$$\begin{cases} (\text{curl } \mathbf{v}_h, \text{curl } \mathbf{w}_h)_P + (\mathbf{w}_h, \nabla \lambda_h)_P = 0, & \forall \mathbf{w}_h \in \mathcal{ND}_{h,0}(\mathcal{T}_h(P)), \\ (\mathbf{v}_h, \nabla p_h) = 0, & \forall p_h \in S_{h,0}(\mathcal{T}_h(P)). \end{cases} \quad (3.5)$$

where $S_{h,0}(\mathcal{T}_h(P))$ is the piecewise linear Lagrange finite element space. Since there is no internal vertex, $S_{h,0}(\mathcal{T}_h(P))$ is a trivial space, and (3.5) reduces to

$$(\text{curl } \mathbf{v}_h, \text{curl } \mathbf{w}_h)_P = 0, \quad \forall \mathbf{w}_h \in \mathcal{ND}_{h,0}(\mathcal{T}_h(P)). \quad (3.6)$$

The fact that $\text{curl } \mathbf{v}_h$ is a piecewise constant on $\mathcal{T}_h(P)$ and integration by parts show

$$\sum_{e \in \mathcal{E}_h(P)} [\text{curl } \mathbf{v}_h]_e \int_e \mathbf{w}_h \cdot \mathbf{t}_e ds = 0, \quad \forall \mathbf{w}_h \in \mathcal{ND}_{h,0}(\mathcal{T}_h(P)). \quad (3.7)$$

Therefore, $\text{curl } \mathbf{v}_h$ must be a single constant on all elements in $\mathcal{T}_h(P)$. Namely, the solution space of (3.5) is $V_h(P)$, and the unisolvence follows from the homogeneous boundary condition yielding the zero solution. \square

Remark 3.1. The proof of Lemma 3.2 basically shows that $\mathbf{v}_h \in V_h(P)$ satisfies $\text{div}_h \mathbf{v}_h = 0$ together with (3.6), where div_h is the element-wise div operator. Namely, the functions in the VEM space (3.8) can be treated as a discrete harmonic extension of the boundary conditions $\mathbf{v}_h \cdot \mathbf{t}$ on ∂P while the original virtual space (3.2) is a continuous extension with a pointwise constraint $\text{div } \mathbf{v}_h = 0$. Therefore functions in $\tilde{V}_h(P)$ may not be polynomials while $V_h(P)$ has piecewise polynomial vectors for which the error estimates is relatively easy to establish.

By Lemma 3.1, it is clearly that $K^q = K_1^q \cup K_2^q$ induces such a triangulation satisfying (P1)–(P3). Meanwhile, we would like to remark that the aforementioned setting and the forthcoming analysis in this paper can be easily extended to the case when \mathcal{T}_h^B is a uniform Cartesian grid, on which the interface elements consist either trapezoids, or triangle-pentagon satisfying (P1)–(P3). In the subsequent analysis involving K^q , the space $V_h(K^q)$ ($P = K^q$) is replacing $\tilde{V}_h(K^q)$

$$V_h(K^q) = \{\mathbf{v}_h \in \mathbf{H}(\text{curl}; K^q) : \mathbf{v}_h|_{K_i^q} \in \mathcal{ND}_h(K_i^q), i = 1, 2, \\ \text{curl}(\mathbf{v}_h) \in \mathbb{P}_0(K^q)\}. \quad (3.8)$$

All these triangles on interface elements form a triangulation resolving the interface, and the global $\mathbf{H}(\text{curl})$ -conforming space is defined as

$$V_h = \{\mathbf{v}_h \in \mathbf{H}_0(\text{curl}; \Omega) : \mathbf{v}_h \in \mathcal{ND}_h(K) \text{ on } K \notin \mathcal{T}_h^q, \text{ and } \mathbf{v}_h \in V_h(K) \text{ on } K \in \mathcal{T}_h^q\}. \quad (3.9)$$

As we assume the background mesh \mathcal{T}_h^B is shape regular, the maximum angle condition holds uniformly for the auxiliary mesh \mathcal{T}_h

3.2. Projection and Interpolation Operators

For a general polygon P and $V_h(P)$, the constant curl \mathbf{v}_h in P can be computed by d.o.f. as

$$\text{curl } \mathbf{v}_h = \frac{1}{|P|} \int_P \text{curl } \mathbf{v}_h \, dx = \frac{1}{|P|} \int_{\partial P} \mathbf{v}_h \cdot \mathbf{t} \, ds. \quad (3.10)$$

With $\text{curl } \mathbf{v}_h$ and $\mathbf{v}_h \cdot \mathbf{t}$ known, its L^2 -projection can be computed following [20, 19]. On any elements or edges $\omega \subseteq \Omega$ we define the local L^2 projection $\Pi_\omega : L^2(\omega) \rightarrow [\mathbb{P}_0(\omega)]^2$ such that

$$(\Pi_\omega \mathbf{v}_h, \mathbf{p})_\omega = (\mathbf{v}_h, \mathbf{p})_\omega, \quad \forall \mathbf{p} \in [\mathbb{P}_0(\omega)]^2 \quad (3.11)$$

which is indeed computable according to the d.o.f. of (3.2) [19, Remark 3]. For readers' sake, we recall the procedure here: for each $\mathbf{p} = (p_1, p_2)^\top \in [\mathbb{P}_0(P)]^2$, there exists $\phi_h = -p_2(x_1 - \bar{x}_1) + p_1(x_2 - \bar{x}_2) \in \mathbb{P}_1(P)$, such that $\underline{\text{curl}} \phi_h = \mathbf{p}$, where (\bar{x}_1, \bar{x}_2) is the point in the star-convexity assumption (P3), Therefore

$$\begin{aligned} (\Pi_{K^q} \mathbf{v}_h, \mathbf{p})_P &= (\mathbf{v}_h, \mathbf{p})_P = (\mathbf{v}_h, \underline{\text{curl}} \phi_h)_P \\ &= (\text{curl } \mathbf{v}_h, \phi_h)_P - (\mathbf{v}_h \cdot \mathbf{t}, \phi_h)_{\partial P}. \end{aligned} \quad (3.12)$$

As $\mathbf{v}_h \cdot \mathbf{t}$ is given as d.o.f., and $\text{curl } \mathbf{v}_h$ is constant, we get

$$\Pi_P \mathbf{v}_h = |P|^{-1} ((\mathbf{v}_h \cdot \mathbf{t}, \bar{x}_2 - x_2)_{\partial P}, -(\mathbf{v}_h \cdot \mathbf{t}, \bar{x}_1 - x_1)_{\partial P})^\top, \quad (3.13)$$

in which the integration on ∂P is with respect to $ds(x_1, x_2)$.

Due to the d.o.f. imposed on edges, we can define the interpolation

$$I_P : \mathbf{H}^1(\text{curl}; P) \rightarrow V_h(P), \quad \int_e I_P \mathbf{u} \cdot \mathbf{t} \, ds = \int_e \mathbf{u} \cdot \mathbf{t} \, ds, \quad \forall e \subseteq \partial P. \quad (3.14)$$

We note that if P is a triangle, I_P reduces exactly to the usual edge interpolation operator, and the special one is for other general polygons such as quadrilateral elements K^q where shape functions are from the virtual space $V_h(P)$ in (3.8). Using integration by parts, we get

$$\int_P \text{curl } I_P \mathbf{u} \, dx = \int_P \text{curl } \mathbf{u} \, dx.$$

Namely $\text{curl } I_P \mathbf{u}$ is the L^2 -projection of $\text{curl } \mathbf{u}$ to the space of constants.

Moreover the interpolation $I_P : \tilde{V}_h(P) \rightarrow V_h(P)$ serves as a bijective mapping which also preserves curl values and the L^2 projection onto $[\mathbb{P}_0(P)]^2$ as both $\tilde{V}_h(P)$

and $V_h(P)$ share the same d.o.f. . For the considered mesh \mathcal{T}_h , taking $P = K \in \mathcal{T}_h$, we have \tilde{V}_h and V_h lead to the same numerical scheme but the analysis based on V_h can exploit more existing tools built for simplicial finite elements.

Finally, a global interpolant \mathbf{u}_I is formed by gluing these local interpolations together, for which certain modification must be introduced on the interface edges forming Γ_h (see Section 5.2).

In the rest of this section, we present some estimates which show the convenience in analysis of opting for the space $V_h(P)$. For a triangle with vertices \mathbf{a}_i , let θ_i be the angle at vertex \mathbf{a}_i and e_i be the edge opposite to \mathbf{a}_i , for $i = 1, 2, 3$.

Lemma 3.3. *The following identity holds for any linear ϕ_h on a triangle T :*

$$\|\nabla \phi_h\|_{L^2(T)}^2 = R_T \sum_{i=1}^3 \cos \theta_i \|\nabla \phi_h \cdot \mathbf{t}_i\|_{L^2(e_i)}^2, \quad (3.15)$$

where R_T is the circumradius of T and \mathbf{t}_i is a unit tangential vector of e_i .

Proof. Denote by $\phi_i := \phi_h(\mathbf{a}_i)$ for $i = 1, 2, 3$. The cotangent formula [12] reads

$$\|\nabla \phi_h\|_{L^2(T)}^2 = \frac{1}{2} \sum_{i=1}^3 \cot \theta_i (\phi_{i-1} - \phi_{i+1})^2.$$

Then the law of sines and $|\nabla \phi_h \cdot \mathbf{t}_i|^2 = (\phi_{i-1} - \phi_{i+1})^2 / |e_i|^2$ finish the proof. \square

We now prove the following Poincaré-type inequality which is the key for the analysis on anisotropic meshes.

Lemma 3.4. *Let P be a simple polygon satisfying (P1)–(P3), then*

$$\|\mathbf{v}_h\|_{L^2(P)} \lesssim h_P^{1/2} \|\mathbf{v}_h \cdot \mathbf{t}\|_{L^2(\partial P)} + h_P \|\operatorname{curl} \mathbf{v}_h\|_{L^2(P)}, \quad \mathbf{v}_h \in V_h(P). \quad (3.16)$$

Proof. Define an auxiliary function

$$\mathbf{w}_h = \frac{\operatorname{curl} \mathbf{v}_h}{2} \begin{bmatrix} -(x_2 - \bar{x}_2) \\ x_1 - \bar{x}_1 \end{bmatrix},$$

where (\bar{x}_1, \bar{x}_2) is the point in the star-convexity condition in (P3). It is clearly that

$$\|\mathbf{w}_h\|_{L^2(P)} \lesssim h_P \|\operatorname{curl} \mathbf{v}_h\|_{L^2(P)}. \quad (3.17)$$

In addition, for every edge $e \in \partial P$, $(-(x_2 - \bar{x}_2), x_1 - \bar{x}_1)^\top \cdot \mathbf{t}|_e$ yields the height l_e of e in the triangle formed by e and (\bar{x}_1, \bar{x}_2) , thus we have $|\mathbf{w}_h \cdot \mathbf{t}|_e = l_e |\operatorname{curl} \mathbf{v}_h|/2$. Together with the star-convexity condition, we have

$$\|\mathbf{w}_h \cdot \mathbf{t}\|_{L^2(e)} \lesssim h_e^{1/2} l_e |\operatorname{curl} \mathbf{v}_h| \lesssim h_P^{1/2} \|\operatorname{curl} \mathbf{v}_h\|_{L^2(P)}. \quad (3.18)$$

Note that $\operatorname{curl}(\mathbf{w}_h - \mathbf{v}_h) = 0$, then by a standard argument of the conforming exact sequence, there exists a continuous piecewise linear finite element function ϕ_h s.t.

$\mathbf{v}_h - \mathbf{w}_h = \nabla \phi_h$. Applying Lemma 3.3, together with the maximum angle condition in (P1), we get the estimate

$$\|\mathbf{v}_h - \mathbf{w}_h\|_{L^2(P)}^2 \lesssim h_P \sum_{e \in \mathcal{E}_h(P)} \|(\mathbf{v}_h - \mathbf{w}_h) \cdot \mathbf{t}_e\|_e^2. \quad (3.19)$$

We then control the norm contribution from an interior edge e . Since P is simply connected, any interior edge e divides P into two parts. Choose the part with less boundary edges and denote it by P_e . Note that $\int_{\partial P_e} \nabla \phi_h \cdot \mathbf{t} \, ds = 0$, consequently by $\nabla \phi_h \cdot \mathbf{t}$ being a constant on each edge on ∂P_e , we have an identity decomposing $\partial P_e = (\partial P_e \cap \partial P) \cup e$,

$$|e| \nabla \phi_h \cdot \mathbf{t}_e + \sum_{e_i \subset \partial P \cap \partial P_e} |e_i| \nabla \phi_h \cdot \mathbf{t}_{e_i} = 0,$$

and thus

$$\|\nabla \phi_h \cdot \mathbf{t}\|_{L^2(e)} \leq \sum_{e_i \subset \partial P \cap \partial P_e} \left(\frac{|e_i|}{|e|} \right)^{1/2} \|\nabla \phi_h \cdot \mathbf{t}_{e_i}\|_{L^2(e_i)}.$$

Then from (3.19) and the condition (P2) we can get

$$\|\mathbf{v}_h - \mathbf{w}_h\|_{L^2(P)}^2 \lesssim h_P \sum_{e \subset \partial P} \left(\|\mathbf{v}_h \cdot \mathbf{t}_e\|_{L^2(e)}^2 + \|\mathbf{w}_h \cdot \mathbf{t}_e\|_{L^2(e)}^2 \right),$$

with constant depending on the number of vertices of P but not the shape regularity of P . Finally, the desired estimate (3.16) follows from the triangle inequality and estimates (3.17)-(3.18). \square

4. A VEM Scheme and An Error Bound

In this section, we describe the proposed virtual element formulation and derive an error bound. We start with the standard weak formulation: find $\mathbf{u} \in \mathbf{H}_0(\text{curl}, \Omega)$ such that

$$a(\mathbf{u}, \mathbf{v}) := (\alpha \, \text{curl} \, \mathbf{u}, \text{curl} \, \mathbf{v})_\Omega + (\beta \, \mathbf{u}, \mathbf{v})_\Omega = (\mathbf{f}, \mathbf{v})_\Omega, \quad \forall \mathbf{v} \in \mathbf{H}_0(\text{curl}, \Omega). \quad (4.1)$$

4.1. A Galerkin method

We emphasize that the local “virtual” element space (3.8) and the global one (3.9) is right away a computable space, readily used for the discretization, unlike (3.2). The d.o.f. on the diagonal edge can be determined by solving (3.6) explicitly, and a set of modified harmonic bases on boundary edges can be obtained and used in computation. As a result, the standard Galerkin formulation is computable without referring to the VEM framework of a projection-stabilization split: find $\mathbf{u}_h \in V_h$ such that

$$(\alpha_h \, \text{curl} \, \mathbf{u}_h, \text{curl} \, \mathbf{v}_h)_\Omega + (\beta_h \, \mathbf{u}_h, \mathbf{v}_h)_\Omega = (\mathbf{f}, \mathbf{v}_h)_\Omega, \quad \mathbf{v}_h \in V_h, \quad (4.2)$$

where α_h and β_h are the modification of α and β according to the linearly approximated interface Γ_h . No projection operator is required since all the shape functions are computable.

However, this approach will introduce an extra partition which becomes inefficient especially in 3D. Instead, we shall treat henceforth the interface part of \mathcal{T}_h as a virtual mesh only appearing in analysis not computation, whereas this associates the meaning of “virtual” in V_h . Its approximation capabilities will be discussed in Section 5.1 based on the maximum angle condition.

4.2. A VEM scheme

Using the L^2 -projection (3.11), we define a bilinear form

$$a_h(\mathbf{u}, \mathbf{v}) := (\alpha_h \operatorname{curl} \mathbf{u}, \operatorname{curl} \mathbf{v})_\Omega + (\beta_h \Pi_h \mathbf{u}, \Pi_h \mathbf{v})_\Omega + \sum_{K \in \mathcal{T}_h^{Bi}} S_K(\mathbf{u}, \mathbf{v}) \quad (4.3)$$

where the operator Π_h is taken as Π_{K^q} if $K = K^q \in \mathcal{T}_h^q$, and the identity operator otherwise. The stabilization $S_K(\mathbf{u}_h, \mathbf{v}_h)$ is defined element-wisely only on $K^q \in \mathcal{T}_h^q$, i.e., the quadrilateral subelements of the interface elements $K \in \mathcal{T}_h^{Bi}$:

$$S_K(\mathbf{u}, \mathbf{v}) = \gamma_K h_K (\beta_h(\mathbf{u} - \Pi_{K^q} \mathbf{u}) \cdot \mathbf{t}, (\mathbf{v} - \Pi_{K^q} \mathbf{v}) \cdot \mathbf{t})_{\partial K^q} \quad (4.4)$$

with a parameter γ_K independent of the mesh size and specified later. Note that the motivation of this stabilization term comes from the approximation of $(\beta_h(\mathbf{u}_h - \Pi_h \mathbf{u}_h), \mathbf{v}_h - \Pi_h \mathbf{v}_h)_{K^q}$ and thus suggests the scaling h_K in (4.4).

At last, the proposed VEM discretization is to find $\mathbf{u}_h \in V_h$ such that

$$a_h(\mathbf{u}_h, \mathbf{v}_h) = (\mathbf{f}, \Pi_h \mathbf{v}_h)_\Omega, \quad \forall \mathbf{v}_h \in V_h. \quad (4.5)$$

4.3. An Error Bound

As mentioned in Section 3, some elements could be extremely anisotropic, and the commonly used norm equivalence in the VEM framework may not be applicable. Following the approach in [9], we shall work on an induced norm on V_h by the bilinear form in (4.3) (Lemma 4.1) which is weaker than the original graph norm:

$$\begin{aligned} \|\mathbf{v}_h\|_h^2 &:= \|\alpha_h^{1/2} \operatorname{curl} \mathbf{v}_h\|_{L^2(\Omega)}^2 + \|\beta_h^{1/2} \Pi_h \mathbf{v}_h\|_{L^2(\Omega)}^2 \\ &\quad + \sum_{K \in \mathcal{T}_h^{Bi}} h_K \|(\mathbf{v}_h - \Pi_{K^q} \mathbf{v}_h) \cdot \mathbf{t}\|_{L^2(\partial K^q)}^2. \end{aligned} \quad (4.6)$$

Lemma 4.1. $\|\cdot\|_h$ defines a norm on V_h .

Proof. Suppose $\|\mathbf{v}_h\|_h = 0$, then clearly $\mathbf{v}_h = \mathbf{0}$ on all triangular elements in \mathcal{T}_h . So we only need to consider $K^q \in \mathcal{T}_h^q$. Indeed, $\Pi_{K^q} \mathbf{v} \equiv \mathbf{0}$ on K^q and $(\mathbf{v}_h - \Pi_{K^q} \mathbf{v}_h) \cdot \mathbf{t}$ vanishing on ∂K^q implies $\mathbf{v}_h \cdot \mathbf{t} = 0$ on ∂K^q . Due to the unisolvence, we have $\mathbf{v}_h = \mathbf{0}$ on K^q which finishes the proof. \square

In the following main theorem, we derive an error equation to (4.5) to demonstrate how the VEM framework can in a novel manner overcome the difficulties of the non-conformity issue aforementioned in the introduction for other DG-based approaches. To reinstate the optimal rate of convergence, we need to further assume that the source term \mathbf{f} bears certain extra local regularity. First, the error is decomposed and the error equation is for $\boldsymbol{\eta}_h$:

$$\mathbf{u} - \mathbf{u}_h = \boldsymbol{\xi}_h + \boldsymbol{\eta}_h, \quad \text{where} \quad \boldsymbol{\xi}_h = \mathbf{u} - \mathbf{u}_I, \quad \text{and} \quad \boldsymbol{\eta}_h = \mathbf{u}_I - \mathbf{u}_h, \quad (4.7)$$

where $\mathbf{u}_I \in V_h$ is an arbitrary function in VEM space.

Theorem 4.1. *Assume that $\mathbf{f} \in L^2(\Omega)$ is locally in \mathbf{H}^1 around the interface, namely $\mathbf{f} \in \mathbf{H}^1(K^q)$ on each $K^q \in \mathcal{T}_h^q$, assume $\mathbf{u} \in \mathbf{H}^1(\text{curl}; \Omega^- \cup \Omega^+)$ is the solution to (4.1) and let $\mathbf{u}_I \in V_h$ be an arbitrary function in VEM space, then for $\boldsymbol{\eta}_h = \mathbf{u}_h - \mathbf{u}_I \in V_h$:*

$$\begin{aligned} \|\boldsymbol{\eta}_h\|_h &\lesssim \left(\sum_{K^q \in \mathcal{T}_h^q} h_K |\mathbf{f}|_{H^1(K^q)} + \sum_{K^q \in \mathcal{T}_h^q} h_K^{1/2} \|(\mathbf{u} - \Pi_h \mathbf{u}_I) \cdot \mathbf{t}\|_{L^2(\partial K^q)} \right. \\ &\quad \left. + \|\alpha \text{curl} \mathbf{u} - \alpha_h \text{curl} \mathbf{u}_I\|_{L^2(\Omega^\pm)} + \|\beta \mathbf{u} - \beta_h \Pi_h \mathbf{u}_I\|_{L^2(\Omega)} \right). \end{aligned} \quad (4.8)$$

Proof. We have

$$a_h(\mathbf{u}_h, \boldsymbol{\eta}_h) - a_h(\mathbf{u}_I, \boldsymbol{\eta}_h) = \underbrace{(\mathbf{f}, \Pi_h \boldsymbol{\eta}_h - \boldsymbol{\eta}_h)_\Omega}_{(I)} + \underbrace{(\mathbf{f}, \boldsymbol{\eta}_h)_\Omega - a_h(\mathbf{u}_I, \boldsymbol{\eta}_h)}_{(II)}. \quad (4.9)$$

For (I), on all the triangular elements in \mathcal{T}_h , Π_h reduce to identity operators, so $\Pi_h \boldsymbol{\eta}_h - \boldsymbol{\eta}_h$ simply vanishes. On a quadrilateral element $K^q \in \mathcal{T}_h^q$, by the definition under (4.3), $\Pi_h \boldsymbol{\eta}_h = \Pi_{K^q} \boldsymbol{\eta}_h$, which is the L^2 -projection of $\boldsymbol{\eta}_h$ on K^q . Therefore

$$\begin{aligned} (\mathbf{f}, \Pi_{K^q} \boldsymbol{\eta}_h - \boldsymbol{\eta}_h)_{K^q} &= (\mathbf{f} - \Pi_{K^q} \mathbf{f}, \Pi_{K^q} \boldsymbol{\eta}_h - \boldsymbol{\eta}_h)_{K^q} \\ &\lesssim h_K |\mathbf{f}|_{H^1(K^q)} \|\Pi_{K^q} \boldsymbol{\eta}_h - \boldsymbol{\eta}_h\|_{L^2(K^q)}. \end{aligned} \quad (4.10)$$

For the term (II) in (4.9), using $\alpha \text{curl} \text{curl} \mathbf{u} + \beta \mathbf{u} = \mathbf{f}$, we have

$$\begin{aligned} (II) &= \underbrace{(\alpha \text{curl} \text{curl} \mathbf{u}, \boldsymbol{\eta}_h)_\Omega - (\alpha_h \text{curl} \mathbf{u}_I, \text{curl} \boldsymbol{\eta}_h)_\Omega}_{(IIa)} \\ &\quad + \underbrace{(\beta \mathbf{u}, \boldsymbol{\eta}_h)_\Omega - (\beta_h \Pi_h \mathbf{u}_I, \Pi_h \boldsymbol{\eta}_h)_\Omega}_{(IIb)} - \underbrace{\sum_{K \in \mathcal{T}_h^{Bi}} S_K(\mathbf{u}_I, \boldsymbol{\eta}_h)}_{(IIc)}. \end{aligned} \quad (4.11)$$

For (IIa), since $\boldsymbol{\eta}_h$ is in the conforming auxiliary space V_h in (3.9), using the integration by parts, the continuity condition of the original PDE, and the curl condition in (3.8) we immediately have

$$\begin{aligned} (IIa) &= (\alpha \text{curl} \mathbf{u}, \text{curl} \boldsymbol{\eta}_h)_\Omega - (\alpha_h \text{curl} \mathbf{u}_I, \text{curl} \boldsymbol{\eta}_h)_\Omega \\ &\leq \|\alpha \text{curl} \mathbf{u} - \alpha_h \text{curl} \mathbf{u}_I\|_{L^2(\Omega)} \|\text{curl} \boldsymbol{\eta}_h\|_{L^2(\Omega)}. \end{aligned} \quad (4.12)$$

For (IIb), on a triangular element K^t , we note that

$$(\beta_h \Pi_h \mathbf{u}_I, \Pi_h \boldsymbol{\eta}_h)_{K^t} = (\beta_h \mathbf{u}_I, \boldsymbol{\eta}_h)_{K^t}. \quad (4.13)$$

On a quadrilateral element K^q , by (3.11) we have

$$(\beta_h \Pi_{K^q} \mathbf{u}_I, \Pi_{K^q} \boldsymbol{\eta}_h)_{K^q} = (\beta_h \Pi_{K^q} \mathbf{u}_I, \boldsymbol{\eta}_h)_{K^q}. \quad (4.14)$$

Combining (4.13) and (4.14), we have

$$(IIb) = (\beta \mathbf{u} - \beta_h \Pi_h \mathbf{u}_I, \boldsymbol{\eta}_h)_\Omega \leq \|\beta \mathbf{u} - \beta_h \Pi_h \mathbf{u}_I\|_{L^2(\Omega)} \|\boldsymbol{\eta}_h\|_{L^2(\Omega)}. \quad (4.15)$$

In addition, for the stabilization term (IIc), by $(\boldsymbol{\eta}_h - \Pi_{K^q} \boldsymbol{\eta}_h) \cdot \mathbf{t}_e \in \mathbb{P}_0(e)$ on each $e \subseteq \partial K^q$ and the definition of the interpolant in (3.14), we have

$$\begin{aligned} S_K(\mathbf{u}_I, \boldsymbol{\eta}_h) &= h_K \int_{\partial K^q} (\mathbf{u}_I - \Pi_{K^q} \mathbf{u}_I) \cdot \mathbf{t} (\boldsymbol{\eta}_h - \Pi_{K^q} \boldsymbol{\eta}_h) \cdot \mathbf{t} \, ds \\ &= h_K \int_{\partial K^q} (\mathbf{u} - \Pi_{K^q} \mathbf{u}_I) \cdot \mathbf{t} (\boldsymbol{\eta}_h - \Pi_{K^q} \boldsymbol{\eta}_h) \cdot \mathbf{t} \, ds \\ &\leq h_K \|(\mathbf{u} - \Pi_{K^q} \mathbf{u}_I) \cdot \mathbf{t}\|_{L^2(\partial K^q)} \|(\boldsymbol{\eta}_h - \Pi_{K^q} \boldsymbol{\eta}_h) \cdot \mathbf{t}\|_{L^2(\partial K^q)}. \end{aligned} \quad (4.16)$$

Finally, putting the estimates in (4.10)-(4.16) to (4.9) yields the following bound

$$\begin{aligned} \|\boldsymbol{\eta}_h\|_h^2 &\lesssim \left(\sum_{K^q \in \mathcal{T}_h^q} h_K |f|_{H^1(K^q)} + \sum_{K^q \in \mathcal{T}_h^q} h_K^{1/2} \|(\mathbf{u} - \Pi_h \mathbf{u}_I) \cdot \mathbf{t}\|_{L^2(\partial K^q)} \right. \\ &\quad \left. + \|\alpha \operatorname{curl} \mathbf{u} - \alpha_h \operatorname{curl} \mathbf{u}_I\|_{L^2(\Omega)} + \|\beta \mathbf{u} - \beta_h \Pi_h \mathbf{u}_I\|_{L^2(\Omega)} \right) \\ &\quad \cdot \left(\sum_{K^q \in \mathcal{T}_h^q} \|\Pi_{K^q} \boldsymbol{\eta}_h - \boldsymbol{\eta}_h\|_{L^2(K^q)} + \|\operatorname{curl} \boldsymbol{\eta}_h\|_{L^2(\Omega)} + \|\boldsymbol{\eta}_h\|_{L^2(\Omega)} \right). \end{aligned} \quad (4.17)$$

To bound $\|\Pi_{K^q} \boldsymbol{\eta}_h - \boldsymbol{\eta}_h\|_{L^2(K^q)}$ on quadrilateral elements, using Lemma 3.4 yields the following estimate

$$\|\Pi_{K^q} \boldsymbol{\eta}_h - \boldsymbol{\eta}_h\|_{L^2(K^q)} \lesssim h_K^{1/2} \|(\Pi_{K^q} \boldsymbol{\eta}_h - \boldsymbol{\eta}_h) \cdot \mathbf{t}\|_{L^2(K^q)} + h_K \|\operatorname{curl} \boldsymbol{\eta}_h\|_{L^2(K^q)}.$$

Putting the estimate above into (4.17) and canceling one $\|\boldsymbol{\eta}_h\|$ on both sides yield the desired result. \square

5. Interpolation Error Estimates

In this section, we estimate the interpolation errors and projection errors of virtual element spaces. Given any triangle T , the interpolation in (3.14) exactly becomes the canonical edge interpolation [38]. If T is further assumed to be shape regular, then the following standard optimal approximation capability holds:

$$\|\mathbf{u} - I_T \mathbf{u}\|_{\mathbf{H}(\operatorname{curl}; T)} \lesssim h_T \|\mathbf{u}\|_{\mathbf{H}^1(\operatorname{curl}; T)}, \quad \mathbf{u} \in \mathbf{H}^1(\operatorname{curl}; T). \quad (5.1)$$

5.1. Estimates based on the Maximum Angle Condition

Due to the assumption of the interface being smooth, we note that certain elements in \mathcal{T}_h^t may inevitably have high aspect ratio in the process of mesh refining, which results that the commonly assumed shape regularity does not hold anymore. Consequently, the standard results about the approximation results of the edge interpolation (5.1) cannot be directly applied. However, since maximum angles of triangles in the auxiliary triangulation around the interface are uniformly bounded if the background mesh is shape regular, the interpolation error estimates can nevertheless be established based on the maximum angle condition. The interpolation estimates based on the maximum angle condition have been long studied for Lagrange elements [3, 32], Raviart-Thomas elements [1, 6, 36], and 3D Nédélec elements [6].

Lemma 5.1 (the same argument as in [1]). *Given any triangle T , let θ_T be the maximum angle of T , then*

$$\|\mathbf{u} - I_T \mathbf{u}\|_{\mathbf{H}(\text{curl}; T)} \lesssim \frac{h_K}{\sin(\theta_T)} \|\mathbf{u}\|_{\mathbf{H}^1(\text{curl}; T)}, \quad \mathbf{u} \in \mathbf{H}^1(\text{curl}; T). \quad (5.2)$$

The results above can be directly applied to estimate the interpolation errors of the virtual space $V_h(K^q)$ on $K^q \in \mathcal{T}_h^q$. Again we present in a more general setting.

Lemma 5.2. *Let P be a simple polygon satisfying (P1)–(P2) and let $I_P \mathbf{u}$ be the edge interpolation to $V_h(P)$ defined in (3.14). Then*

$$\|\mathbf{u} - I_P \mathbf{u}\|_{\mathbf{H}(\text{curl}; P)} \lesssim h_P \|\mathbf{u}\|_{\mathbf{H}^1(\text{curl}; \text{Conv}(P))}, \quad \mathbf{u} \in \mathbf{H}^1(\text{curl}; \text{Conv}(P)). \quad (5.3)$$

Proof. The estimate for the semi-curl norm is standard since $\text{curl } I_P \mathbf{u}$ is the L^2 projection of $\text{curl } \mathbf{u}$ on P . Then

$$\begin{aligned} \|\text{curl } \mathbf{u} - \text{curl } I_P \mathbf{u}\|_{L^2(P)} &= \|\text{curl } \mathbf{u} - \Pi_P \text{curl } \mathbf{u}\|_{L^2(P)} \\ &\leq \|\text{curl } \mathbf{u} - \Pi_{\text{Conv}(P)} \text{curl } \mathbf{u}\|_{L^2(P)} \\ &\leq \|\text{curl } \mathbf{u} - \Pi_{\text{Conv}(P)} \text{curl } \mathbf{u}\|_{L^2(\text{Conv}(P))} \\ &\leq \frac{h_P}{\pi} \|\mathbf{u}\|_{\mathbf{H}^1(\text{curl}; \text{Conv}(P))}, \end{aligned}$$

where the last step is the Poincaré inequality over convex domains [40].

Let I_h be the edge interpolation to $V_h(\mathcal{T}_h(P))$, i.e., the standard edge finite element space on mesh $\mathcal{T}_h(P)$. By the maximum angle condition in (P1) and Lemma 5.1, we have $\|\mathbf{u} - I_h \mathbf{u}\|_{L^2(P)} \lesssim h_P \|\mathbf{u}\|_{\mathbf{H}^1(\text{curl}; P)}$. Then it suffices to estimate the difference $\|I_P \mathbf{u} - I_h \mathbf{u}\|_{L^2(K)}$ on each triangle $K \in \mathcal{T}_h(P)$. We apply Lemma 3.4 on each K to get

$$\|I_P \mathbf{u} - I_h \mathbf{u}\|_{L^2(K)} \leq \sum_{e \subset \partial K} h_K^{1/2} \|(I_P \mathbf{u} - I_h \mathbf{u}) \cdot \mathbf{t}\|_{L^2(e)} + h_K \|\text{curl}(I_P \mathbf{u} - I_h \mathbf{u})\|_{L^2(K)}.$$

As $(I_P \mathbf{u} - I_h \mathbf{u}) \cdot \mathbf{t} = 0$ for $e \subset \partial P$, we only consider an interior edge e . Since P is simple, any interior edge e divides P into two parts. Choose the part with less

boundary edges and denoted by P_e , then we have the relation

$$|e|(I_P \mathbf{u} - I_h \mathbf{u}) \cdot \mathbf{t}_e = \int_{P_e} \operatorname{curl}(I_P \mathbf{u} - I_h \mathbf{u}) \, dx,$$

which can be used to get

$$|e|^{1/2} \|(I_P \mathbf{u} - I_h \mathbf{u}) \cdot \mathbf{t}\|_{L^2(e)} \leq \|\operatorname{curl}(I_P \mathbf{u} - I_h \mathbf{u})\|_{L^2(P_e)} |P_e|^{1/2}.$$

Using the triangle inequality, together with the estimates for $\operatorname{curl}(\mathbf{u} - I_P \mathbf{u})$ and $\operatorname{curl}(\mathbf{u} - I_h \mathbf{u})$, we conclude for any $K \in \mathcal{T}_h(P)$

$$\|I_P \mathbf{u} - I_h \mathbf{u}\|_{L^2(K)} \lesssim h_P^2 \|\operatorname{curl} \mathbf{u}\|_{H^1(\operatorname{Conv}(P))}. \quad (5.4)$$

The desired result (5.3) then follows from the triangle inequality. \square

5.2. An Interface-aware Interpolation

In the interpolation error estimate, locally a norm $\|\operatorname{curl} \mathbf{u}\|_{H^1(K)}$ will be used. When K is an interface element, in general $\operatorname{curl} \mathbf{u} \notin H^1(K)$ but in $H^1(K^+ \cup K^-)$. Instead we will use the fact $\operatorname{curl} \mathbf{u}_E^\pm \in H^1(K)$ and define the interpolation by the tangential components of either \mathbf{u}_E^+ or \mathbf{u}_E^- , where which extension to use depends on the measure of K^- and K^+ . Note that, in the present situation, since both the triangular elements in \mathcal{T}_h^t and the quadrilateral elements in \mathcal{T}_h^q may have high aspect ratio, the modification in [26] may not be suitable on anisotropic meshes with interface being present. Therefore, we shall employ a different interface-aware interpolation.

In the following discussion, we only present the results for the elements in the mesh \mathcal{T}_h due to the technical treatment for the interface. But we emphasize that most of the results can be generalized based on the estimate of the interpolation errors on general polygons above. We shall use K to denote an interface element in \mathcal{T}_h^B that is cut into K_h^- and K_h^+ by the edge Γ_h^K , and without loss of generality, we assume $K_h^- \in \mathcal{T}_h^t$ and $K_h^+ \in \mathcal{T}_h^q$. Recall that K_{int} is the portion sandwiched between Γ and Γ_h^K , and we further define $K_{\text{int}}^\pm := K_h^\pm \cap K_{\text{int}}$ which is equivalent to $K_h^\pm \cap K^\mp$, namely the mismatching subregions of K_h^\pm as shown in Figure 5.1. Let \mathcal{E}_K be the collection of edges of K_h^- and K_h^+ but excluding the edge Γ_h^K . We define a modified interpolation operator \tilde{I}_K on $K \in \mathcal{T}_h^{Bi}$ such that

$$\int_e \tilde{I}_K \mathbf{u} \cdot \mathbf{t} \, ds = \int_e \mathbf{u} \cdot \mathbf{t} \, ds, \quad \forall e \in \mathcal{E}_K, \quad (5.5a)$$

$$\int_{\Gamma_h^K} \tilde{I}_K \mathbf{u} \cdot \mathbf{t} \, ds = \begin{cases} \int_{\Gamma_h^K} \mathbf{u}_E^+ \cdot \mathbf{t} \, ds, & \text{if } |K_h^+| \leq |K_h^-|, \\ \int_{\Gamma_h^K} \mathbf{u}_E^- \cdot \mathbf{t} \, ds, & \text{if } |K_h^-| < |K_h^+|. \end{cases} \quad (5.5b)$$

By such a definition, we can always keep the interpolation as the standard one on the subelement with smaller size. So when estimation on the mismatch portion is needed, such as (5.15), the element size appearing on the denominator will be

always larger than $|K|/2$ such that the overall estimate can be controlled. This consideration serves as our key motivation to make this modification. For simplicity, we denote \mathbf{u}_I by the global interpolant such that

$$\mathbf{u}_I = I_K \mathbf{u} \quad \text{if } K \notin \mathcal{T}_h^{Bi} \quad \text{and} \quad \mathbf{u}_I = \tilde{I}_K \mathbf{u} \quad \text{if } K \in \mathcal{T}_h^{Bi}.$$

In addition, we use $I_{K_h^\pm} \mathbf{u}_E^\pm$ to denote the canonical interpolation on K_h^\pm for Sobolev extensions \mathbf{u}_E^\pm . We emphasize that the modified \tilde{I}_K serves the purpose for the error analysis and is not needed in actual computation.

The following two lemmas are presented for general polygons. So we temporarily let K be an interface polygon, and the notation Γ^K , Γ_h^K and K_{int} are all defined in the same manner as their counterparts for triangular interface elements. For the subelement with larger size, inevitably there is a mismatch on Γ_h^K , so these results are essential. In the following discussion, with slightly abuse of the notations, we denote $\tilde{h}_K = |\Gamma_h^K|$ which might be much smaller than h_K (see Fig. 5.1 (left)), and $\|\mathbf{u}_E^\pm\|_{L^2(K)} := \|\mathbf{u}_E^-\|_{L^2(K)} + \|\mathbf{u}_E^+\|_{L^2(K)}$ with trivial generalization to other Sobolev norms.

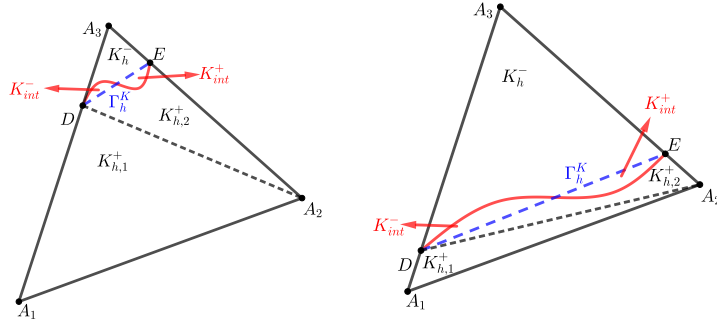


Fig. 5.1. Left: the triangular interface is the smaller one. Right: the quadrilateral element is the smaller one.

The edge Γ_h^K is assumed to be part in Ω^+ and part in Ω^- . As a result, the line integral $\int_{\Gamma_h^K} \mathbf{u} \cdot \mathbf{t} ds$ has part of the integrand being $\mathbf{u}_E^+ \cdot \mathbf{t}$ while the other being $\mathbf{u}_E^- \cdot \mathbf{t}$. Their difference appears one of the key terms to bound the error of the modified interpolant (5.5), as one adheres to one extension in defining the interpolation.

Lemma 5.3. *Let $\mathbf{u} \in \mathbf{H}^1(\text{curl}; \Omega^- \cup \Omega^+)$. Given an interface polygon K , there holds*

$$\left| \int_{\Gamma_h^K} (\mathbf{u}_E^+ - \mathbf{u}_E^-) \cdot \mathbf{t} ds \right| \lesssim \tilde{h}_K^{1/2} h_K \|\text{curl } \mathbf{u}_E^\pm\|_{L^2(K_{\text{int}})}. \quad (5.6)$$

Proof. Applying integration by parts on K_{int} and using the jump condition in

(1.1c), we obtain

$$\left| \int_{\Gamma_h^K} (\mathbf{u}_E^+ - \mathbf{u}_E^-) \cdot \mathbf{t} \, ds \right| = \left| \int_{K_{\text{int}}} \text{curl}(\mathbf{u}_E^+ - \mathbf{u}_E^-) \, ds \right| \lesssim |K_{\text{int}}|^{1/2} \|\text{curl} \, \mathbf{u}_E^\pm\|_{L^2(K_{\text{int}})}$$

which yields (5.6) since $|K_{\text{int}}| \lesssim \tilde{h}_K h_K^2$ by (2.1). \square

The result above can be used to derive the following trace inequality. Recall that there exists a shape regular triangle $B_h^K \subseteq \Omega$ with the base Γ_h^K and a height $\mathcal{O}(h_K)$ by Assumption (B) for all interface elements.

Lemma 5.4. *Let $\mathbf{u} \in \mathbf{H}^1(\text{curl}; \Omega^- \cup \Omega^+)$. Given an interface polygon K with Γ_h^K , there holds*

$$\|(\mathbf{u}_E^+ - \mathbf{u}_E^-) \cdot \mathbf{t}\|_{L^2(\Gamma_h^K)} \lesssim h_K^{1/2} \|\mathbf{u}_E^\pm\|_{H^1(B_h^K)} + h_K \|\text{curl} \, \mathbf{u}_E^\pm\|_{L^2(K_{\text{int}})}. \quad (5.7)$$

Proof. Apply the L^2 -projection on Γ_h^K to obtain

$$\begin{aligned} \|(\mathbf{u}_E^- - \mathbf{u}_E^+) \cdot \mathbf{t}\|_{L^2(\Gamma_h^K)} &\leq \underbrace{\|(\mathbf{u}_E^- - \mathbf{u}_E^+) \cdot \mathbf{t} - \Pi_{\Gamma_h^K}((\mathbf{u}_E^- - \mathbf{u}_E^+) \cdot \mathbf{t})\|_{L^2(\Gamma_h^K)}}_{\text{(I)}} \\ &\quad + \underbrace{\|\Pi_{\Gamma_h^K}((\mathbf{u}_E^- - \mathbf{u}_E^+) \cdot \mathbf{t})\|_{L^2(\Gamma_h^K)}}_{\text{(II)}}. \end{aligned} \quad (5.8)$$

Since \mathbf{t} is a constant vector and Γ_h^K with B_h^K satisfies the height condition, by the trace inequality [9, Lemma 6.3] and Poincaré inequality with average zero on a boundary edge [9, Lemma 6.11], we have

$$\begin{aligned} \text{(I)} &\lesssim l^{-1/2} \|(\mathbf{u}_E^- - \mathbf{u}_E^+) \cdot \mathbf{t} - \Pi_{\Gamma_h^K}((\mathbf{u}_E^- - \mathbf{u}_E^+) \cdot \mathbf{t})\|_{L^2(B_h^K)} \\ &\quad + (l^{1/2} + l^{-1/2} \tilde{h}_K) \|(\mathbf{u}_E^- - \mathbf{u}_E^+) \cdot \mathbf{t}\|_{H^1(B_h^K)} \\ &\lesssim h_K^{1/2} \|(\mathbf{u}_E^- - \mathbf{u}_E^+) \cdot \mathbf{t}\|_{H^1(B_h^K)}. \end{aligned} \quad (5.9)$$

For (II), by Lemma 5.3, we have

$$\begin{aligned} \text{(II)} &= \tilde{h}_K^{1/2} \left| \Pi_{\Gamma_h^K}((\mathbf{u}_E^- - \mathbf{u}_E^+) \cdot \mathbf{t}) \right| \\ &= \tilde{h}_K^{-1/2} \left| \int_{\tilde{e}} (\mathbf{u}_E^- - \mathbf{u}_E^+) \cdot \mathbf{t} \, ds \right| \lesssim h_K \|\text{curl} \, \mathbf{u}_E^\pm\|_{L^2(K_{\text{int}})}. \end{aligned} \quad (5.10)$$

Putting (5.9) and (5.10) back into (5.8) finishes the proof. \square

5.3. Estimate on Interface Elements

Now we proceed to estimate the interpolation errors $\mathbf{u} - \mathbf{u}_I$ on interface elements for the modified interpolation.

Lemma 5.5. *Let $\mathbf{u} \in \mathbf{H}^1(\text{curl}; \Omega^- \cup \Omega^+)$. Given each interface element $K \in \mathcal{T}_h^{Bi}$, there holds*

$$\|\mathbf{u} - \mathbf{u}_I\|_{\mathbf{H}(\text{curl}; K)} \lesssim h_K \|\mathbf{u}_E^\pm\|_{\mathbf{H}^1(\text{curl}; K \cup B_h^K)} + \|\mathbf{u}_E^\pm\|_{\mathbf{H}(\text{curl}; K_{\text{int}})}. \quad (5.11)$$

Proof. Recall that $K = K_h^- \cup K_h^+$. Without loss of generality, we focus the proof on K_h^- as the estimate on the other part follows the result on K_h^- using a similar argument as the one in Lemma 5.2. By the triangle inequality, we have

$$\|\mathbf{u} - \mathbf{u}_I\|_{\mathbf{H}(\text{curl}; K_h^-)} \leq \|\mathbf{u} - \mathbf{u}_E^-\|_{\mathbf{H}(\text{curl}; K_h^-)} \quad (\text{I})$$

$$+ \|\mathbf{u}_E^- - I_{K_h^-} \mathbf{u}_E^-\|_{\mathbf{H}(\text{curl}; K_h^-)} \quad (\text{II})$$

$$+ \|I_{K_h^-} \mathbf{u}_E^- - \mathbf{u}_I\|_{\mathbf{H}(\text{curl}; K_h^-)}. \quad (\text{III})$$

The first term (I) can be bounded by

$$\|\mathbf{u} - \mathbf{u}_E^-\|_{\mathbf{H}(\text{curl}; K_h^-)} = \|\mathbf{u}_E^+ - \mathbf{u}_E^-\|_{\mathbf{H}(\text{curl}; K_{\text{int}}^-)} \leq \|\mathbf{u}_E^\pm\|_{\mathbf{H}(\text{curl}; K_{\text{int}})}, \quad (5.12)$$

and the second term (II) directly follows from Lemma 5.1 since the triangular element K_h^- satisfies the maximum angle condition. The third term (III) simply vanishes if $|K_h^-| \leq |K_h^+|$, therefore the estimate for this term is only needed when $|K_h^-| > |K_h^+|$ and consequently $|K_h^-| \geq Ch_K^2$. For simplicity, we let $\mathbf{w}_h = I_{K_h^-} \mathbf{u}_E^- - \mathbf{u}_I$, and note that $\mathbf{w}_h \cdot \mathbf{t}$ vanishes on the edges of K_h^- except Γ_h^K . Using integration by parts and Lemma 5.3, we have

$$\|\text{curl } \mathbf{w}_h\|_{L^2(K_h^-)} = |K_h^-|^{1/2} |\text{curl } \mathbf{w}_h| = \frac{1}{|K_h^-|^{1/2}} \left| \int_{\Gamma_h^K} \mathbf{w}_h \cdot \mathbf{t} \, ds \right| \quad (5.13)$$

$$\lesssim \frac{1}{h_K} \left| \int_{\Gamma_h^K} (\mathbf{u}_E^- - \mathbf{u}_E^+) \cdot \mathbf{t} \, ds \right| \lesssim h_K^{1/2} \|\text{curl } \mathbf{u}_E^\pm\|_{L^2(K_{\text{int}})}. \quad (5.14)$$

To estimate the L^2 -norm, we use inequality (3.16) in Lemma 3.4 to conclude

$$\|\mathbf{w}_h\|_{L^2(K_h^-)} \lesssim h_K^{1/2} \|\mathbf{w}_h \cdot \mathbf{t}\|_{L^2(\Gamma_h^K)} + h_K \|\text{curl } \mathbf{w}_h\|_{L^2(K_h^-)}. \quad (5.15)$$

Lastly, using Lemma 5.4 and the bound of $\|\text{curl } \mathbf{w}_h\|_{L^2(K_h^-)}$ finishes the proof. \square

The estimates on non-interface elements in the background mesh \mathcal{T}_h^B are standard. These estimates together with the Sobolev inequality in Lemma 2.2 and Theorem 2.1 on the extension yield the global interpolation estimate.

Theorem 5.1. *Let $\mathbf{u} \in \mathbf{H}^1(\text{curl}; \Omega^- \cup \Omega^+)$, then there holds*

$$\|\mathbf{u} - \mathbf{u}_I\|_{\mathbf{H}(\text{curl}; \Omega)} \lesssim h \|\mathbf{u}\|_{\mathbf{H}^1(\text{curl}; \Omega^- \cup \Omega^+)}. \quad (5.16)$$

Proof. For non-interface elements, the estimate is standard as well. For interface element K , we then use Lemma 5.5:

$$\begin{aligned} \sum_{K \in \mathcal{T}_h^{Bi}} \|\mathbf{u} - \mathbf{u}_I\|_{\mathbf{H}(\text{curl}; K)}^2 &\lesssim \sum_{K \in \mathcal{T}_h^{Bi}} h_K^2 \|\mathbf{u}_E^\pm\|_{\mathbf{H}^1(\text{curl}; K \cup B_h^K)}^2 + \|\mathbf{u}_E^\pm\|_{\mathbf{H}(\text{curl}; K_{\text{int}})}^2, \\ &\lesssim h^2 \|\mathbf{u}_E^\pm\|_{\mathbf{H}^1(\text{curl}; \Omega^- \cup \Omega^+)}^2 + \|\mathbf{u}_E^\pm\|_{\mathbf{H}(\text{curl}; \cup_{K \in \mathcal{T}_h^{Bi}} K_{\text{int}})}^2, \end{aligned}$$

in which the second step we use the fact Γ_h is uniform Lipschitz so that the overlapping portions of triangles B_h^K for every interface element K are bounded. The desired estimate follows from Theorem 2.1 and estimate (2.4). \square

5.4. Estimate on the stabilization

In this subsection, we move back to the mesh \mathcal{T}_h consisting of triangular and quadrilateral elements cut from the background triangular mesh. On the quadrilateral K_h^+ , a stabilization term is present. In this section such terms appearing in the error bound are estimated, including

$$\|(\mathbf{u} - \mathbf{u}_I) \cdot \mathbf{t}\|_{L^2(\partial K)}, \quad \|\Pi_{K^q}(\mathbf{u} - \mathbf{u}_I) \cdot \mathbf{t}\|_{L^2(\partial K)}, \quad \|(\mathbf{u} - \Pi_{K^q} \mathbf{u}_I) \cdot \mathbf{t}\|_{L^2(\partial K)}.$$

The main difficulty is on the second term above. Note that the common and natural approach to estimate the edge terms is to apply the trace inequality, which indeed works for the edges A_1D and A_2E due to the corresponding $\mathcal{O}(h_K)$ height within the triangle. However, the major difficulty arises for edges like A_1A_2 and $\Gamma_h^K = DE$, due to a possibly degenerating height. The core idea of our approach is to employ a constructive proof, without relying on the trace inequality, to control the edge terms by using $\Pi_{K^q}(\mathbf{u} - \mathbf{u}_I) \cdot \mathbf{t}$ being a constant for lifting and applying the definition of projection (3.12). In the coming proofs, $\boldsymbol{\xi}_h := \mathbf{u} - \mathbf{u}_I$ for simplicity.

Lemma 5.6. *Let $\mathbf{u} \in \mathbf{H}^1(\text{curl}; \Omega^- \cup \Omega^+)$. Given each interface element $K \in \mathcal{T}_h^{Bi}$, there holds*

$$\|(\mathbf{u} - \mathbf{u}_I) \cdot \mathbf{t}\|_{L^2(\partial K_h^+)} \lesssim h_K^{1/2} \|\mathbf{u}_E^\pm\|_{H^1(K)} + h_K \|\text{curl } \mathbf{u}_E^\pm\|_{L^2(K_{\text{int}})}. \quad (5.17)$$

Proof.

First, we have on each edge $e \neq \Gamma_h^K \subseteq \partial K_h^+$, $\int_e \boldsymbol{\xi}_h \cdot \mathbf{t} \, ds = 0$, and thus

$$\|\boldsymbol{\xi}_h \cdot \mathbf{t}\|_{L^2(e)} \lesssim h_e^{1/2} |\mathbf{u} \cdot \mathbf{t}|_{H^{1/2}(e)} \leq Ch_K^{1/2} \|\mathbf{u}_E^+\|_{H^1(K)}, \quad (5.18)$$

where we have used the fact that e is one part of an edge of the regular element K such that the trace inequality can be applied on this edge and K . On Γ_h^K , by the triangle inequality, we have

$$\begin{aligned} \|\boldsymbol{\xi}_h \cdot \mathbf{t}\|_{L^2(\Gamma_h^K)} &\leq \|(\mathbf{u} - \mathbf{u}_E^+) \cdot \mathbf{t}\|_{L^2(\Gamma_h^K)} \\ &\quad + \|(\mathbf{u}_E^+ - I_{K_h^+} \mathbf{u}_E^+) \cdot \mathbf{t}\|_{L^2(\Gamma_h^K)} + \|(I_{K_h^+} \mathbf{u}_E^+ - \mathbf{u}_I) \cdot \mathbf{t}\|_{L^2(\Gamma_h^K)}. \end{aligned} \quad (5.19)$$

For the first term in (5.19), note that

$$\|(\mathbf{u} - \mathbf{u}_E^+) \cdot \mathbf{t}\|_{L^2(\Gamma_h^K)} \leq \|(\mathbf{u}_E^- - \mathbf{u}_E^+) \cdot \mathbf{t}\|_{L^2(\Gamma_h^K)} \quad (5.20)$$

of which the estimate follows from Lemma 5.4. The second term in (5.19) follows from the argument similar to (5.18).

The third term in (5.19) simply vanishes when $|K_h^+| < |K_h^-|$. If $|K_h^+| \geq |K_h^-|$, then the estimate follows from Lemma 5.3. \square

Lemma 5.7. *Let $\mathbf{u} \in \mathbf{H}^1(\text{curl}; \Omega^- \cup \Omega^+)$. Given each interface element $K \in \mathcal{T}_h^{Bi}$, there holds*

$$\|\Pi_{K_h^+}(\mathbf{u} - \mathbf{u}_I) \cdot \mathbf{t}\|_{L^2(\partial K_h^+)} \lesssim h_K^{1/2} \|\mathbf{u}_E^\pm\|_{\mathbf{H}^1(\text{curl}; K)} + h_K^{-1/2} \|\mathbf{u}_E^\pm\|_{\mathbf{H}(\text{curl}; K_{\text{int}})}. \quad (5.21)$$

Proof. For simplicity, we assume A_1 is at the origin, K is contained in the first quadrant, and the edge A_1A_2 aligns with the x -axis having a tangential vector $(1, 0)^\top$. Let e be an edge of K_h^+ with the unit tangential vector \mathbf{t}_e . If $e = A_1D$ or A_2E , since the height within K_h^+ with respect to these two edges cannot degenerate, a simple scaling directly leads to

$$\|\Pi_{K_h^+} \boldsymbol{\xi}_h \cdot \mathbf{t}\|_{L^2(e)} \lesssim h_K^{-1/2} \|\Pi_{K_h^+} \boldsymbol{\xi}_h\|_{L^2(K_h^+)} \leq h_K^{-1/2} \|\boldsymbol{\xi}_h\|_{L^2(K_h^+)},$$

and then the estimate follows from Lemma 5.5. For $e = A_1A_2$ or DE , if both $|A_1D| \geq \gamma|A_1A_3|$ and $|A_2E| \geq \gamma|A_2A_3|$, with a constant $\gamma \in (0, 1)$ bounded away from 0, the trace inequality-based argument above can be still applied.

The major difficulty is how to deal with edges $e = A_1A_2$ or DE when K_h^+ becomes degenerate. Without loss of generality, we assume $|A_1D| \leq |A_1A_3|/2$ or $|A_2E| \leq |A_2A_3|/2$ (see Figure 5.1 (right) for an illustration). In such a case, $|DE| \gtrsim h_K$ independent of the interface location thanks to the law of sines as either $|A_3D| \geq |A_1A_3|/2$ or $|A_3E| \geq |A_2A_3|/2$. Now let $D = (r_1, r_2)$ and $E = (s_1, s_2)$, we have

$$ch_K \max\{r_2, s_2\} \leq |K_h^+| \leq Ch_K \max\{r_2, s_2\}. \quad (5.22)$$

Next, $p_h^e \in \mathbb{P}_1(K_h^+)$ is sought such that $\text{curl} p_h^e = \mathbf{t}_e$. Since $\Pi_{K_h^+} \boldsymbol{\xi}_h$ is a constant, and by (3.12), we have

$$\begin{aligned} \|\Pi_{K_h^+} \boldsymbol{\xi}_h \cdot \mathbf{t}_e\|_{L^2(e)} &= \frac{h_e^{1/2}}{|K_h^+|} \left| (\Pi_{K_h^+} \boldsymbol{\xi}_h, \text{curl} p_h^e)_{K_h^+} \right| \\ &\leq \underbrace{\frac{h_e^{1/2}}{|K_h^+|} \left| (\text{curl} \boldsymbol{\xi}_h, p_h^e)_{K_h^+} \right|}_{\text{(I)}} + \underbrace{\frac{h_e^{1/2}}{|K_h^+|} \left| (\boldsymbol{\xi}_h \cdot \mathbf{t}, p_h^e)_{L^2(\partial K_h^+)} \right|}_{\text{(II)}}. \end{aligned} \quad (5.23)$$

If $e = A_1A_2$, then $\mathbf{t}_e = (1, 0)^\top$, and $p_h^e = y$ which implies $\|p_h^e\|_{L^\infty(K_h^+)} \leq \max\{r_2, s_2\}$. If $e = DE$, then

$$\mathbf{t}_e = \frac{(r_1 - s_1, r_2 - s_2)}{|DE|}, \quad \text{and} \quad p_h^e = \frac{(r_1 - s_1)x_2 - (r_2 - s_2)x_1}{|DE|}.$$

Note that $|(r_1 - s_1)x_2| \lesssim h_K \max\{r_2, s_2\}$ and $|(r_2 - s_2)x_1| \lesssim h_K \max\{r_2, s_2\}$, as a result, the following estimate always holds

$$\|p_h^e\|_{L^\infty(K_h^+)} \lesssim \max\{r_2, s_2\}. \quad (5.24)$$

Now we proceed to estimate (I) and (II) individually. For (I), by (5.22) and (5.24) there holds

$$\|p_h^e\|_{L^2(K_h^+)} \lesssim \max\{r_2, s_2\} |K_h^+|^{1/2} \lesssim |K_h^+|^{3/2} h_K^{-1}.$$

Therefore,

$$\text{(I)} \lesssim |K_h^+|^{1/2} h_K^{-1/2} \|\text{curl} \boldsymbol{\xi}_h\|_{L^2(K_h^+)} \lesssim h_K^{1/2} \|\text{curl} \boldsymbol{\xi}_h\|_{L^2(K_h^+)} \quad (5.25)$$

of which the estimate follows from Lemma 5.5. For (II), on each $e' \subseteq \partial K_h^+$ using (5.22) and (5.24) again, we have

$$\|p_h^e\|_{L^2(e')} \lesssim \max\{r_2, s_2\} h_{e'}^{1/2} \lesssim |K_h^+| h_K^{-1/2}.$$

Lastly, we arrive at

$$(II) \leq \frac{h_e^{1/2}}{|K_h^+|} \|\boldsymbol{\xi}_h \cdot \mathbf{t}\|_{L^2(\partial K_h^+)} \|p_h^e\|_{L^2(\partial K_h^+)} \lesssim \|\boldsymbol{\xi}_h \cdot \mathbf{t}\|_{L^2(\partial K_h^+)} \quad (5.26)$$

of which the estimate follows from Lemma 5.6. Putting (5.25) and (5.26) into (5.23) finishes the proof. \square

Lemma 5.8. *Let $\mathbf{u} \in \mathbf{H}^1(\text{curl}; \Omega^- \cup \Omega^+)$. Given each interface element $K \in \mathcal{T}_h^{Bi}$, there holds*

$$\|(\mathbf{u} - \Pi_{K_h^+} \mathbf{u}_I) \cdot \mathbf{t}\|_{L^2(\partial K_h^+)} \lesssim h_K^{1/2} \|\mathbf{u}_E^\pm\|_{\mathbf{H}^1(\text{curl}; K)} + h_K^{-1/2} \|\text{curl } \mathbf{u}_E^\pm\|_{L^2(K_{\text{int}})}. \quad (5.27)$$

Proof. Let us decompose the error into

$$\begin{aligned} & \|(\mathbf{u} - \Pi_{K_h^+} \mathbf{u}_I) \cdot \mathbf{t}\|_{L^2(\partial K_h^+)} \\ & \leq \|(\mathbf{u} - \Pi_{K_h^+} \mathbf{u}_E^+) \cdot \mathbf{t}\|_{L^2(\partial K_h^+)} + \|(\Pi_{K_h^+} \mathbf{u}_E^+ - \Pi_{K_h^+} \mathbf{u}_I) \cdot \mathbf{t}\|_{L^2(\partial K_h^+)}. \end{aligned} \quad (5.28)$$

Here the estimate of the second term is similar to the one in Lemma 5.7. Therefore, we only need to estimate the first term in (5.28) which is further decomposed into

$$\begin{aligned} & \|(\mathbf{u} - \Pi_{K_h^+} \mathbf{u}_E^+) \cdot \mathbf{t}\|_{L^2(\partial K_h^+)} \\ & \leq \underbrace{\|(\mathbf{u} - \mathbf{u}_E^+) \cdot \mathbf{t}\|_{L^2(\partial K_h^+)}}_{(I)} + \underbrace{\|(\mathbf{u}_E^+ - \Pi_{K_h^+} \mathbf{u}_E^+) \cdot \mathbf{t}\|_{L^2(\partial K_h^+)}}_{(II)}. \end{aligned} \quad (5.29)$$

Note that (I) is only non-zero on Γ_h^K of which the estimate follows from Lemma 5.4. For (II), if $e \subseteq \partial K_h^+$ is A_1D or A_2E , i.e., it has an $\mathcal{O}(h_K)$ height within K_h^+ . Then we apply the trace inequality [9, Lemma 6.3] and the approximation result of the L^2 projection to obtain

$$(II) \lesssim h_K^{-1/2} \|\mathbf{u}_E^+ - \Pi_{K_h^+} \mathbf{u}_E^+\|_{L^2(K_h^+)} \lesssim h_K^{1/2} \|\mathbf{u}_E^+\|_{H^1(K_h^+)}.$$

If $e \subseteq \partial K_h^+$ is A_1A_2 or DE where the corresponding height may become degenerate, we first apply the trace inequality on the whole shape-regular element K , and then apply the Poincaré inequality [9, Lemma 5.3], to obtain

$$(II) \lesssim h_K^{-1/2} \|\mathbf{u}_E^+ - \Pi_{K_h^+} \mathbf{u}_E^+\|_{L^2(K)} \lesssim h_K^{1/2} \|\mathbf{u}_E^+\|_{H^1(K)}.$$

Combining the estimates above finishes the proof. \square

6. Convergence Analysis

In this section, based on the previous results, we estimate the convergence order of the solution errors. In particular, we need to estimate each term in the error bound (6.2). Our main task is to estimate those terms on quadrilateral elements. In the following discussion, we still keep our notation that $K_h^+ \in \mathcal{T}_h^q$ will be the quadrilateral subelement associated with each interface element $K \in \mathcal{T}_h^{Bi}$.

Theorem 6.1 (An a priori convergence result for VEM). *Under the same assumption of Theorem 4.1, let $\mathbf{u} \in \mathbf{H}^1(\text{curl}; \Omega^- \cup \Omega^+)$ and let the background mesh \mathcal{T}_h^B satisfy the assumptions (A) and (B), then the solution \mathbf{u}_h to the VEM scheme (4.5) admits the error estimates*

$$\|\mathbf{u} - \mathbf{u}_h\|_{H(\text{curl}; \Omega)} \lesssim h \|\mathbf{u}\|_{\mathbf{H}^1(\text{curl}; \Omega^+ \cup \Omega^-)} + h \sum_{K^q \in \mathcal{T}_h^q} |f|_{H^1(K^q)}. \quad (6.1)$$

Proof. First of all, by the triangle inequality, we have

$$\|\mathbf{u} - \mathbf{u}_h\|_{H(\text{curl}; \Omega)} \leq \|\mathbf{u} - \mathbf{u}_I\|_{H(\text{curl}; \Omega)} + \|\mathbf{u}_I - \mathbf{u}_h\|_{H(\text{curl}; \Omega)}.$$

Recall $\boldsymbol{\eta}_h = \mathbf{u}_I - \mathbf{u}_h$. We use Lemma 3.4 to obtain

$$\begin{aligned} \sum_{K \in \mathcal{T}_h} \|\boldsymbol{\eta}_h\|_K^2 &\leq \sum_{K \in \mathcal{T}_h} \|\Pi_h \boldsymbol{\eta}_h\|_K^2 + \|(I - \Pi_h) \boldsymbol{\eta}_h\|_K^2 \\ &\lesssim \sum_{K \in \mathcal{T}_h} \|\Pi_h \boldsymbol{\eta}_h\|_K^2 + h_K \|(I - \Pi_h) \boldsymbol{\eta}_h \cdot \mathbf{t}\|_{\partial K}^2 + h_K^2 \|\text{curl } \boldsymbol{\eta}_h\|_K^2 \\ &\lesssim \|\boldsymbol{\eta}_h\|_h^2 \end{aligned}$$

Recall that in Theorem 4.1, we have obtained

$$\begin{aligned} \|\boldsymbol{\eta}_h\|_h &\lesssim \left(\sum_{K^q \in \mathcal{T}_h^q} h_K |f|_{H^1(K^q)} + \sum_{K^q \in \mathcal{T}_h^q} h_K^{1/2} \|(\mathbf{u} - \Pi_h \mathbf{u}_I) \cdot \mathbf{t}\|_{L^2(\partial K^q)} \right. \\ &\quad \left. + \|\alpha \text{curl } \mathbf{u} - \alpha_h \text{curl } \mathbf{u}_I\|_{L^2(\Omega^\pm)} + \|\beta \mathbf{u} - \beta_h \Pi_h \mathbf{u}_I\|_{L^2(\Omega)} \right). \end{aligned} \quad (6.2)$$

Then the estimate follows from Lemma 5.8 and Theorem 5.1, and applying a simple triangle inequality to the last term. \square

7. Numerical Examples

In this section, we present a group of numerical experiments to validate the previous estimates. Let the computation domain be $\Omega = (-1, 1) \times (-1, 1)$, and background mesh be generated by triangulating an $N \times N$ Cartesian mesh by cutting each square into two triangles along its diagonal. We highlight that the proposed method can be used on any other regular background triangular meshes. A circular interface $\{\Gamma : x^2 + y^2 = r_1^2\}$ cuts Ω into the inside subdomain Ω^- and the outside subdomain

Ω^+ . We consider the example in [24, 34] that the exact solution is

$$\mathbf{u} = \begin{cases} \begin{pmatrix} \mu^- (-k_1(r_1^2 - x^2 - y^2)y) \\ \mu^- (-k_1(r_1^2 - x^2 - y^2)x) \end{pmatrix} & \text{in } \Omega^-, \\ \begin{pmatrix} \mu^+ (-k_2(r_2^2 - x^2 - y^2)(r_1^2 - x^2 - y^2)y) \\ \mu^+ (-k_2(r_2^2 - x^2 - y^2)(r_1^2 - x^2 - y^2)x) \end{pmatrix} & \text{in } \Omega^+, \end{cases} \quad (7.1)$$

where the boundary conditions and the right hand side \mathbf{f} are calculated accordingly. We employ the parameters $k_2 = 20$, $k_1 = k_2(r_2^2 - r_1^2)$ with $r_1 = \pi/5$ and $r_2 = 1$, and fix $\alpha^- = \beta^- = 1$ with varying $\alpha^+ = 10$ or 100 and $\beta^+ = 10$ or 100. For simplicity, we define the errors

$$e_0 = \|\mathbf{u} - \mathbf{u}_h\|_{L^2(\Omega)} \quad \text{and} \quad e_1 = \|\text{curl}(\mathbf{u} - \mathbf{u}_h)\|_{L^2(\Omega)}. \quad (7.2)$$

The numerical results are presented in Tables 1-4 which clearly show the first order convergence for both errors.

h	e_0	rate	e_1	rate
1/10	0.6257	NA	1.3893	NA
1/20	0.3258	0.94	0.6998	0.99
1/40	0.1661	0.97	0.3534	0.99
1/80	0.0843	0.98	0.1784	0.99
1/160	0.0424	0.99	0.0894	1.00
1/320	0.0213	1.00	0.0447	1.00
1/640	0.0107	0.99	0.0224	1.00

Table 1. Solution errors for $\alpha^+ = 10$ and $\beta^+ = 10$.

h	e_0	rate	e_1	rate
1/10	0.6206	NA	1.3912	NA
1/20	0.3257	0.93	0.7000	0.99
1/40	0.1661	0.97	0.3534	0.99
1/80	0.0843	0.98	0.1784	0.99
1/160	0.0424	0.99	0.0894	1.00
1/320	0.0213	1.00	0.0447	1.00
1/640	0.0107	1.00	0.0224	1.00

Table 2. Solution errors for $\alpha^+ = 10$ and $\beta^+ = 100$.

h	e_0	rate	e_1	rate
1/10	0.3266	NA	1.0795	NA
1/20	0.1761	0.89	0.5449	0.99
1/40	0.0926	0.93	0.2768	0.98
1/80	0.0482	0.94	0.1406	0.98
1/160	0.0246	0.97	0.0705	1.00
1/320	0.0124	0.99	0.0353	1.00
1/640	0.0062	0.99	0.0177	1.00

Table 3. Solution errors for $\alpha^+ = 100$ and $\beta^+ = 10$.

h	e_0	rate	e_1	rate
1/10	0.1938	NA	0.8877	NA
1/20	0.1425	0.44	0.4358	1.03
1/40	0.0698	1.03	0.1976	1.14
1/80	0.0368	0.92	0.1027	0.95
1/160	0.0189	0.96	0.0503	1.03
1/320	0.0101	0.90	0.0264	0.93
1/640	0.0054	0.91	0.0140	0.92

Table 4. Solution errors for $\alpha^+ = 100$ and $\beta^+ = 100$.

Acknowledgment

This work was supported in part by the National Science Foundation under grants DMS-1913080 and DMS-2012465.

References

1. G. Acosta and R. G. Durán. The maximum angle condition for mixed and non-conforming elements: Application to the Stokes equations. *SIAM J. Numer. Anal.*, 37(1):18–36, 1999. [3](#), [16](#)
2. H. Ammari, A. Buffa, and J.-C. Nédélec. A justification of eddy currents model for the Maxwell equations. *SIAM J. Appl. Math.*, 60(5):1805–1823, 2000. [2](#)
3. I. Babuška and A. K. Aziz. On the angle condition in the finite element method. *SIAM J. Numer. Anal.*, 13(2):214–226, 1976. [16](#)
4. R. Beck, R. Hiptmair, R. H.W. Hoppe, and B. Wohlmuth. Residual based a posteriori error estimators for eddy current computation. *ESAIM Math. Model. Numer. Anal.*, 34(1):159–182, 2000. [2](#)
5. L. Beirão da veiga, F. Brezzi, A. Cangiani, G. Manzini, L. D. Marini, and A. Russo. Basic principles of virtual element methods. *Math. Models Methods Appl. Sci.*, 23(01):199–214, 2013. [3](#)
6. A. Buffa, M. Costabel, and M. Dauge. Algebraic convergence for anisotropic edge elements in polyhedral domains. *Numer. Math.*, 101(1):29–65, 2005. [16](#)
7. E. Burman, S. Claus, P. Hansbo, M. G. Larson, and A. Massing. CutFEM: Discretizing geometry and partial differential equations. *Internat. J. Numer. Methods Engrg.*, 104(7):472–501, 2015. [2](#)
8. Z. Cai and S. Cao. A recovery-based a posteriori error estimator for $H(\text{curl})$ interface problems. *Comput. Methods Appl. Mech. Engrg.*, 296:169 – 195, 2015. [2](#)
9. S. Cao and L. Chen. Anisotropic error estimates of the linear virtual element method on polygonal meshes. *SIAM J. Numer. Anal.*, 56(5):2913–2939, 2018. [3](#), [13](#), [19](#), [23](#)
10. R. Casagrande, R. Hiptmair, and J. Ostrowski. An a priori error estimate for interior penalty discretizations of the curl-curl operator on non-conforming meshes. *J. Math. Ind.*, 6(1):4, 2016. [2](#), [3](#)
11. R. Casagrande, C. Winkelman, R. Hiptmair, and J. Ostrowski. DG treatment of non-conforming interfaces in 3D Curl-Curl problems. In *Scientific Computing in Electrical Engineering*, pages 53–61, Cham, 2016. Springer International Publishing. [2](#), [3](#)
12. L. Chen. Introduction to finite element methods, 2007. [11](#)
13. L. Chen, H. Wei, and M. Wen. An interface-fitted mesh generator and virtual element methods for elliptic interface problems. *J. Comput. Phys.*, 334:327–348, 2017. [3](#), [8](#)
14. Z. Chen, Q. Du, and J. Zou. Finite element methods with matching and nonmatching meshes for Maxwell equations with discontinuous coefficients. *SIAM J. Numer. Anal.*, 37(5):1542–1570, 2000. [2](#)
15. Z. Chen, Z. Wu, and Y. Xiao. An adaptive immersed finite element method with arbitrary Lagrangian-Eulerian scheme for parabolic equations in time variable domains. *Int. J. Numer. Anal. Mod.*, pages 567–591, 2015. [2](#)
16. Z. Chen, Y. Xiao, and L. Zhang. The adaptive immersed interface finite element method for elliptic and Maxwell interface problems. *J. Comput. Phys.*, 228(14):5000 – 5019, 2009. [2](#), [4](#)
17. P. Ciarlet, Jr and J. Zou. Fully discrete finite element approaches for time-dependent Maxwell’s equations. *Numer. Math.*, 82(2):193–219, 1999. [2](#)
18. M. Costabel, M. Dauge, and S. Nicaise. Singularities of Maxwell interface problems. *ESAIM Math. Model. Numer. Anal.*, 33(3):627–649, 1999. [6](#)

19. L. Beirão da Veiga, F. Brezzi, F. Dassi, L.D. Marini, and A. Russo. Virtual element approximation of 2D Magnetostatic problems. *Computer Methods in Applied Mechanics and Engineering*, 327:173 – 195, 2017. Advances in Computational Mechanics and Scientific Computation—the Cutting Edge. [3](#), [4](#), [7](#), [8](#), [10](#)
20. L. Beirão da Veiga, F. Brezzi, L. D. Marini, and A. Russo. H(div) and H(curl)-conforming virtual element methods. *Numer. Math.*, 133(2):303–332, 2016. [3](#), [4](#), [7](#), [8](#), [10](#)
21. L. Beirão da Veiga, F. Dassi, G. Manzini, and L. Mascotto. Virtual elements for Maxwell's equations. [arXiv:2102.00950](#), 2021. [3](#)
22. H. Duan, F. Qiu, R. C. E. Tan, and W. Zheng. An adaptive FEM for a Maxwell interface problem. *J. Sci. Comput.*, 67(2):669–704, 2016. [2](#)
23. R. Guo and T. Lin. A group of immersed finite element spaces for elliptic interface problems. *IMA J.Numer. Anal.*, 39(1):482–511, 2017. [2](#), [5](#), [6](#)
24. R. Guo, Y. Lin, and J. Zou. Solving two dimensional H(curl)-elliptic interface systems with optimal convergence on unfitted meshes. [arXiv:2011.11905](#), 2020. [3](#), [25](#)
25. R. Hiptmair. Finite elements in computational electromagnetism. *Acta Numerica*, 11:237–339, 2002. [2](#)
26. R. Hiptmair, J. Li, and J. Zou. Convergence analysis of finite element methods for H(curl; ω)-elliptic interface problems. *Numer. Math.*, 122(3):557–578, Nov 2012. [2](#), [6](#), [7](#), [17](#)
27. P. Houston, I. Perugia, A. Schneebeli, and D. Schötzau. Interior penalty method for the indefinite time-harmonic Maxwell equations. *Numer. Math.*, 100(3):485–518, 2005. [3](#)
28. P. Houston, I. Perugia, and D. Schotzau. Mixed discontinuous Galerkin approximation of the Maxwell operator. *SIAM J. Numer. Anal.*, 42(1):434–459, 2004. [3](#)
29. P. Houston, I. Perugia, and D. Schötzau. Mixed discontinuous Galerkin approximation of the Maxwell operator: Non-stabilized formulation. *J. Sci. Comput.*, 22(1):315–346, 2005. [3](#)
30. J. Huang and J. Zou. Uniform a priori estimates for elliptic and static Maxwell interface problems. *Disc. Cont. Dynam. Sys., Series B*, 7(1):145, 2007. [6](#)
31. F. Kikuchi. Mixed formulations for finite element analysis of magnetostatic and electrostatic problems. *Japan J. Appl. Math.*, 6(2):209, 1989. [3](#)
32. M. Křížek. On the maximum angle condition for linear tetrahedral elements. *SIAM J. Numer. Anal.*, 29(2):513–520, 1992. [16](#)
33. R. J. LeVeque and Z. Li. The immersed interface method for elliptic equations with discontinuous coefficients and singular sources. *SIAM J. Numer. Anal.*, 31(4):1019–1044, 1994. [2](#)
34. J. Li, J. M. Melenk, B. Wohlmuth, and J. Zou. Optimal a priori estimates for higher order finite elements for elliptic interface problems. *Appl. Numer. Math.*, 60(1):19–37, 2010. [6](#), [25](#)
35. H. Liu, L. Zhang, X. Zhang, and W. Zheng. Interface-penalty finite element methods for interface problems in H^1 , H(curl), and H(div). *Comput. Methods Appl. Mech. Engrg.*, 367, 2020. [2](#)
36. L. D. Marini. An inexpensive method for the evaluation of the solution of the lowest order Raviart–Thomas mixed method. *SIAM J. Numer. Anal.*, 22(3):493–496, 1985. [16](#)
37. P. Monk. Analysis of a finite element method for maxwell's equations. *SIAM J. Numer. Anal.*, 29(3):714–729, 1992. [2](#)
38. P. Monk. *Finite Element Methods for Maxwell's Equations*. Oxford University Press, 2003. [3](#), [15](#)

- 39. J. C. Nédélec. Mixed finite elements in \mathbb{R}^3 . *Numer. Math.*, 35(3):315–341, 1980. [7](#)
- 40. L. E. Payne and H. F. Weinberger. An optimal Poincaré inequality for convex domains. *Arch. Ration. Mech. Anal*, 5(1):286–292, 1960. [16](#)
- 41. K. Roppert, S. Schoder, F. Toth, and M. Kaltenbacher. Non-conforming Nitsche interfaces for edge elements in curl-curl-type problems. *IEEE Trans. Magn.*, 56(5):1–7, May 2020. [3](#)
- 42. H. Wei, L. Chen, Y. Huang, and B. Zheng. Adaptive mesh refinement and superconvergence for two-dimensional interface problems. *SIAM J. Sci. Comput.*, 36(4):A1478–A1499, 2014. [6](#)
- 43. J. Zhao. Analysis of finite element approximation for time-dependent Maxwell problems. *Math. Comp.*, 73(247), 2000. [2](#)
- 44. S. Zhao and G. W. Wei. High-order FDTD methods via derivative matching for Maxwell’s equations with material interfaces. *J. Comput. Phys.*, 200(1):60–103, 2004. [2](#)